Received 13 July 2024, accepted 30 July 2024, date of publication 5 August 2024, date of current version 16 August 2024.

Digital Object Identifier 10.1109/ACCESS.2024.3439021

RESEARCH ARTICLE

Solving Optimal Power Flow Control Problem Using Honey Formation Optimization Algorithm

VOLKAN YAMAÇLI[1], **HAKAN IŞIKER**[2], **(Member, IEEE), ZEKİ YETGİN**[1], **AND KADİR ABACI**[2]

[1]Computer Engineering Department, Faculty of Engineering, Mersin University, 33343 Mersin, Türkiye

[2]Electrical and Electronics Engineering Department, Faculty of Engineering, Mersin University, 33343 Mersin, Türkiye

Corresponding author: Hakan Işiker (hakan.isiker@mersin.edu.tr)

ABSTRACT This paper introduces three new variations of the HFO-1 (Honey Formation Optimization with Single Component) algorithm, namely HFO-1a, HFO-1b and HFO-1c, adapted to address the optimal power flow (OPF) problem. The original HFO-1 algorithm has shown success in solving various numerical problems in recent years; however, it assumes a single search range for all dimensions of the solution space, making it unsuitable for direct application to the OPF problem. Modifications to both the honey formation and mixing phases of the HFO-1 algorithm were made to improve solution quality and convergence speed, resulting in three new variants of HFO-1. The newly developed variants aim to minimize even the most challenging objective functions of the complex OPF problem, which has been further complicated by the integration of renewable energy sources into power systems. The paper provides a comprehensive and transparent comparison of the three types of IEEE 30-bus test systems and 118-bus test systems with existing methods, meticulously adhering to practical, technical, operational, and safety constraints. Following successful results on the CEC 2021 standard benchmark functions, the proposed HFO-1 variants have been thoroughly validated through extensive analysis. Experimental results demonstrate that the proposed approach can achieve lower costs ($800.5972/hour and $800.3871/hour) in two types of IEEE 30-bus systems without integrating renewable resources while maintaining system constraints. Furthermore, HFO-1a (achieving 3.0776261 MW) and HFO-1b achieve the lowest values in the literature with a multi-fuel cost of (646.375893 $/h) and a valve point effective fuel cost of (823.981360 $/h), respectively, while HFO-1c exhibits a voltage deviation of (0.083498 p.u.) and Prohibited Operating Zones (POZ) cost of generator (800.665078 $/h).

INDEX TERMS Optimal power flow, honey formation optimization, HFO-1 variants, practical constraints, renewable energy.

I. INTRODUCTION

A. BACKGROUND AND MOTIVATION

Optimal power flow (OPF) is still a widely discussed topic in power systems since it was proposed in 1962 [1] and defined as OPF by Dommel and Tinney [2]. The primary goal of OPF is to optimize the allocation of generation and transmission resources, considering factors such as power generation costs, line losses, and system reliability. This is achieved by determining the active output powers and voltages of the generators, as well as the reactive power output values of the shunt capacitor banks and the tap settings of the on-load tap changers. The optimal settings of controllable parameters within a power network are determined to achieve specific objectives while satisfying operational constraints. The complexity of OPF is further increased by including variable constraints while optimizing and satisfying the system parameters for the objective functions. The primary goal

The associate editor coordinating the review of this manuscript and approving it for publication was Cuo Zhang.

of optimal power flow is to optimize a specific objective function while satisfying practical, physical, operational, and security constraints.

Moreover, can be further complicated by the addition of different objectives with varying forms, such as a non-convex fuel cost function that takes into account valve point loading effects, a piecewise fuel cost function that takes into account multiple fuel options, and a discrete fuel cost function that takes into account prohibited operating zones. The OPF problem is inherently nonlinear and presents numerous optimal solutions, encompassing local and global optima. When factoring in the uncertainties stemming from the high penetration of renewable energy sources in modern power systems, the complexity of the problem is further compounded. The motivation of this paper is to offer an optimal resolution to this formidable challenge while upholding all system constraints, and to collate the relevant findings from existing literature for a comprehensive and transparent comparison under consistent conditions.

B. LITERATURE REVIEW

In the past, classical numerical optimization methods such as the Gradient-based method [1], non-linear programming [2], gradient projection method [3], linear programming (LP) [4], [5], quadratic programming (QP) [6], Newton-based method [7], [8], sequential unconstrained minimization technique [9] and interior point methods (IPMs) [10] have been widely used. However, these methods have problems such as convexity, continuity assumptions, and a tendency to converge to local optima due to their reliance on gradient-based searches. In fact, the OPF problem is a challenging problem with nonlinearity, different forms and multiple optimal solutions of the objective functions to be minimized. Therefore, traditional methods are not suitable for achieving the global optimum and hardly handle non-differentiable objective functions.

Using meta-heuristic algorithms instead of classical optimization methods has become indispensable in recent years to solve the OPF problem involving multiple independent single-objective functions. In the early stages of solving OPF problems with meta-heuristic approaches, genetic algorithms, and improved genetic algorithms [11], [12], conventional evolutionary programming (EP) [13] gained prominence. In the following years, new versions based on genetic algorithms such as enhanced genetic algorithm (EGA) [14], GA-fuzzy system approach (GA-FSA) [15], EGA with new decomposed quadratic load flow (EGA-DQLF) [16] and improved EP (IEP) [17] were introduced to the literature. In this area, other subsequent methods include differential evolution (DE) [18] and its versions such as self-adaptive differential evolution by augmented Lagrange multiplier method (SADEALM) [19], modified DE (MDE) [20], hybrid differential evolution simulated annealing and tabu search based algorithm (HDE-SATS) [21] and adaptive constrained differential evolution (ACDE) [22] and effective constraint handling techniques differential evolution [23]. References [17] and [18], OPF problems are solved using multiple fuel options, which made some improvements. In [19] and [20], a new penalty method was proposed to search for the best solution during the mutation phase. The work [21] further improved the solution performance and outperformed DE. In [22], a three-stage method was presented for a differential development algorithm, providing an effective solution to power system constraints. In [23], the OPF problem was solved by combining constraint handling (CH) techniques and self-adaptive (SP) penalty functions and integrating them into the differential evolution (ECHT-DE) algorithm. Particle swarm optimization (PSO) [24] algorithm has also been successfully applied to the OPF problem. The global best solution and inertia-weighted PSO (GWPSO) [25], adaptive particle swarm optimization (APSO) [26], evolving ant-directed particle swarm optimization (EADPSO) [27], stochastic weight trade-off particle swarm optimization (SWT-PSO) [28] and parallel metaheuristics for graphics processing units (GPU-PSO) are PSO based methods to solve the OPF problem. In [25], the inertia weighting factor was used to find the best solution quickly. In [26], the solution was reached by updating the weight factors with chaotic formulations. In [27], various models are introduced to improve the convergence speed. In [28], SWT-PSO is presented to improve the algorithm search capabilities by maintaining the balance between global exploration and local exploitation. In [29], a parallel optimal power flow solver, is proposed to run entirely on graphics processing units (GPUs) using a particle swarm optimization (PSO) algorithm.

In addition to the above studies, further developed algorithms for solving the OPF problem can be listed as follows; biogeography-based (BBO), quasi-opposite biogeography-based optimization (QOBBO) and adaptive real coded biogeography-based optimization(ARCBBO) [30], [31], [32], gravity search algorithm (GSA) [33], opposition-based gravity search algorithm (NSMOGSA) [34], non-dominated sorting multi-objective opposition-based gravitational search algorithm (NSMOOGSA) [35], harmony search algorithm (HS) [36], improved harmony search method (IHS) [37], chaotic self-adaptive differential harmony search algorithm CDHS [38], artificial bee colony algorithm (ABC) [39], improved artificial bee colony algorithm (IABC) [40], bacterial foraging algorithm (BFA) [41], teaching-learning based optimization technique (TLBO) [42], modified weighted teaching-learning based optimization (WTLBO) [43], Lévy mutation teaching-learning based optimization (LTLBO) [44] Grey Wolf Optimizer (GWO) [45], cross-search based grey wolf optimizer (CS-GWO) [46], backtracking search algorithm (BSA) [47], search for symbiotic organisms (SOS) [48], breeding krill swarm (SKH) algorithm [49], opposition-based krill swarm algorithm (OKHA) [50],moth flame optimizer (IMFO) [51], JAYA algorithm [52], adaptive multiple teams perturbation-guiding Jaya (AMTG-JAYA) [53], novel Sine-Cosine algorithm (MSCA) [54], moth swarm algorithm (MSA) [55], cross-entropy method with chaotic operator (CGSCE) [56], enhanced computational optimizer of the Social Network Search Technique (ESNST) [57] are used to handle the OPF challenge.

The field of OPF research is expanding with the advent of advanced optimization methods in both machine learning [58] and artificial intelligence, leading to more advanced algorithms with global search abilities [59], such as evolutionary algorithms, swarm algorithms, and other heuristic algorithms [60], [61], [62], [63], [64], [65], [66], [67]. For instance, in [60], a modified crow search optimization tool (MCSO) has been proposed to solve the coupled economic emission power flow (EEPF) problem. In [61] and [62], Salma Abd el-Sattar et al. and Zhu et al. proposed new optimization approaches, namely the Salp swarm algorithm (ISSA) and coyote optimization (COA) algorithm, respectively, to solve the optimal power flow problem. In [63], Manzoor Ahmad et al. used an effective methodology, called Orthogonal Experimental Design (OED), to solve the OPF problem by integrating it with the Bird Swarm Algorithm (IBSA). The OPF problem was successfully solved using the Successive History-based Adaptive Differential Evolutionary (SHADE) algorithm in [64] and the Improved Constrained Adaptive Differential Evolution (ICAD) algorithm in [65]. In [66], Kaur and Narang utilized the space transformational invasive weed optimization (ST-IWO) algorithm, a combination of invasive weed optimization (IWO) and space transformation search (STS) techniques, to address single and multi-objective optimal power flow problems. In [67], Shaheen et al. made two changes to the standard jellyfish search optimizer (JFS) algorithm in their proposed algorithm, called Semi- Quasi-Reflected Jellyfish Search Optimizer (QRJFS). They examined thirteen cases with economic, environmental, and technical objectives in four test systems and showed the superiority of their proposed algorithm. Additionally, the OPF problem is addressed using hybrid algorithms proposed in [68] and [69], namely the Hybrid Approach with Combining Cuckoo Search and Gray Wolf (THCSGWO) and Optimal Power Flow Employing a Hybrid Sine Cosine-Grey Wolf Optimizer (HSC-GWO), respectively. In [70], the Arithmetic Optimization Algorithm (AOA) and Aquila Optimizer (AO) solvers, namely the AO-AOA, are applied to solve the Optimal Power Flow (OPF) problem, where the objective is to independently optimize the generation fuel cost, power loss, emission, voltage deviation, and L index. In [71], a Hybrid Differential Evolution and Harmony Search (Hybrid DE-HS) algorithm has been proposed for the OPF formulation, which includes active and reactive power constraints, prohibited zones, and valve point loading effects of generators. In [72] the FAHSPSO-DE approach is proposed, which combines self-adaptive particle swarm optimization (SPSO) and differential evolution algorithms to efficiently solve the OPF problem for three IEEE standard systems: IEEE 30-, 57-, and 118-bus test systems.

Researchers have developed various modifications and variants to existing algorithms to handle these drawbacks, including modified and combined methods. For example, in [73], Nguyen proposed a new social spider optimization algorithm (NISSO) for the OPF solution by making three changes in the traditional social spider optimization algorithm (SSO) to improve and accelerate the optimal solution quality. In [74], a Modified Artificial Hummingbird Algorithm (MAHA) has been proposed to effectively solve OPF and enhance the performance of the original Artificial Hummingbird Algorithm. In [75], a new variant of the Animal Migration Optimization (AMO) algorithm, known as Boundary Allocation Animal Migration Optimization (BA-AMO), was conceptualized to study the optimal power flow problem associated with IEEE bus systems. In literature, there are various studies aforementioned on the OPF of traditional power systems by using such methods of employ numerical or heuristic approaches. But since the usage and integration of renewable energy systems to power system increases drastically in recent years, OPF studies have been directed towards another goal which is optimizing the power system while being fed by unpredictable renewable energy sources of PV and wind. The best planning for an isolated hybrid power system with a PV system, a diesel generator, and battery storage has been discussed in [76]. Another study, the alternating current OPF problem for thermal, wind, solar, and tidal energy systems have been resolved by using the symbiotic organisms search [77]. Also, the dynamic economic dispatch optimization issue has taken into account the emission and valve-point loading influence of the generator [77]. In addition to these studies, renewable related and highly-focused OPF studies take consideration of stochastic wind power and energy [78]. Another study on hydrothermal-wind scheduling of hybrid power systems carried out for optimal results [79]. And, multi-objective optimization of wind energy integrated power systems is achieved in terms of cost and system parameters in [80].

C. RESEARCH GAP AND CONTRIBUTIONS

Considering the non-linear and convex nature of the optimal power flow (OPF) problem, as well as the current economic situation, increasing global energy demand, technological advancements, and the challenges associated with the growing integration of renewable resources into power systems, finding optimal solutions using proposed algorithms requires substantial time and effort in the research field. Researchers commonly rely on IEEE test systems to assess the accuracy and performance of proposed algorithms. However, there are many studies in which control and state variables have different numbers in the same test system [73], [81], [82], [83], [84], [85], solution interval values of variables and constraints are different [42], [44], [46], [54], [64], [71], [75], variables are unverifiable because they are not reported [51], [66], [69], [72], [86], different coefficients are preferred for the same objective functions [64], [87], [88]. Furthermore, many studies even do not provide sufficient results or search ranges for the variables such that validations of their feasibilities are not possible. The works in literature generally blindly compare various optimization algorithms in achieving the OPF problem by using different search ranges (lower and upper limits) for the same variables (solution variables or constraint variables). Since the methods are not transparent enough, it is also not possible to verify their feasibility. Sorting through the literature and identifying those OPF applications having exactly the same test conditions is a challenging process. Therefore, this study will inspire researchers by highlighting that no single approach will be sufficient in OPF studies. The proposed methods should be compared with systems under the same test conditions.

Recently, honey formation optimization (HFO) framework [89] was proposed by Yetgin and colleagues for solving mathematical problems where the formulations of the objective functions are known or designed. HFO extends the Artificial Bee Colony (ABC) algorithm with the concept of multiple components in a source and the worker bees tending to collect components currently needed. However, the necessity of component design for a particular problem makes the HFO not applicable to optimize an arbitrary objective function. In [90], HFO with a single component (HFO-1) has been proposed by Yetgin and colleagues to remove this hardship of HFO for numerical function optimizations. HFO-1 is original in that it extends the formation phase of HFO with novel local search and, importantly, introduces three new phases, mixing, maturation, and saturation, specific to honey production, but it needs modification to solve the challenging OPF problem. Three modifications were made to solve the OPF problem using the HFO-1 algorithm: HFO-1a, HFO-1b, and HFO-1c. The performance of these modifications was then tested using 12 benchmark functions from CEC 2021. For simplicity, the original HFO-1 assumes a fixed bound range (lower and upper limit) for all parameter values. This mainly creates a problem in the mixing phase of HFO-1 that randomly mixes parameter values across different dimensions. In order to get rid of this limitation HFO-1a and HFO-1b are proposed. Furthermore, the honey formation phase of the HFO-1 is not open to vectorial implementation due to each bee sequentially updating the visited sources. Thus, HFO-1c is further proposed to improve the honey formation phase. This article not only adapts the HFO-1 algorithm to solve the challenging OPF problem by developing variants of the proposed HFO-1 algorithm for the solution of mathematical problems but also uses it to solve an engineering problem for the first time.

The main contributions of this paper as follows,

- A novel optimization method whose performance is shown with benchmark studies is applied to engineering problem for the first time.
- It is shown that by applying small parameter changes to HFO framework, the chance of converging to better solution sets can be achieved.
- The proposed algorithm that has different variants which shows better performance depending on the study case of three type modification IEEE-30 and 118 bus test systems.
- The performance of the proposed approach is compared with results of recent state-of-art studies compromised in literature. The obtained results show that the proposed approach not only can optimize the system better than most of the studies but also can keep the system in constraints.

The paper is organized as follows: Section II presents the mathematical formulation of the OPF problem and summarizes the objective functions. Section III provides an overview of the Honey Formation Optimization for Single Component (HFO-1) and its variants. The first subsection of Section IV discusses test studies on 12 CEC 2021 benchmark functions of the proposed HFO-1 variants. The second subsection provides a detailed description of OPF studies and compares simulation results. Conclusions are drawn in Section V.

II. OPTIMAL POWER FLOW

The main objective of the OPF problem considered in this study is to minimize the objective functions such as prohibited and non-prohibited valve effect and non-valve effect generation cost, active power loss, and voltage deviation while keeping the variables such as generation bus voltage magnitudes, load bus voltage magnitudes, shunt VAR capacitances, and transformer tap settings within the constraint limits.

The problem can be defined as:

Optimize: $f(x, u)$

With the subject of: $g(x, u) = 0$ and $h(x, u) \leq 0$

In accordance with

$$u = [P_{Gslack} V_L \; Q_G S_{TL}] \tag{1}$$

where u indicates the state variables, including real generation power of the slack bus P_{Gslack}, voltage of the load bus V_L, reactive generation power Q_G and transmission line loading S_{TL}

$$x = \left[\, P_G \; V_G \; Q_C \; T \,\right] \tag{2}$$

where x represents the variable vector for the elements, including the real power P_G, generator voltage V_G, the output of shunt VAR compensators Q_C and settings of the tap changing transformers T, f *and* g represent the objective function and the load flow equations, respectively, h indicates the parameter limits of the system.

A. EQUALITY AND INEQUALITY CONSTRAINTS OF THE POWER SYSTEM

1) EQUALITY CONSTRAINTS

The typical equations related to load flow, $g(x, u)$, in the literature, is given by,

$$P_{G_i} - P_{D_i} - \sum\nolimits_{j=1}^{n} |V_i| \left|V_j\right| \left|Y_{ij}\right| cos\left(\theta_{ij} - \delta_i + \delta_j\right) = 0 \tag{3}$$

$$Q_{G_i} - Q_{D_i} - \sum_{j=1}^{n} |V_i| \left|V_j\right| \left|Y_{ij}\right| sin\left(\theta_{ij} - \delta_i + \delta_j\right) = 0 \tag{4}$$

where P_{Gi} and Q_{Gi} are the real and reactive generation power outputs, P_{Di} and Q_{Di} are the active load and reactive load demand of bus i, the bus admittance matrix elements are represented by θ_{ij}, and finally, n is the total bus number.

2) INEQUALITY CONSTRAINTS

These constraints h(x, u,) limit the security of the power system and are categorized as follows:

Active, reactive power outputs and bus voltages of the generators are restricted by their lower and upper limits, and the formulations of generator constraints are given as follows,

$$V_{Gi}^{min} \leq V_{Gi} \leq V_{Gi}^{max}, \quad i = 1, \ \ldots\ldots, N_g \tag{5.a}$$
$$P_{Gi}^{min} \leq P_{Gi} \leq P_{Gi}^{max}, \quad i = 1, \ \ldots\ldots, N_g \tag{5.b}$$
$$Q_{Gi}^{min} \leq Q_{Gi} \leq Q_{Gi}^{max}, \quad i = 1, \ \ldots\ldots., N_g \tag{5.c}$$

where N_g defines the number of generators, including the slack bus.

The maximum and minimum limits of tap settings regarding the transformer is given by,

$$T_i^{min} \leq T_i \leq T_i^{max}, \quad i = 1 \ldots\ldots\ldots, N_T \tag{6}$$

The maximum and minimum reactive power that can be injected or absorbed by compensators are defined by the user as,

$$Q_{C_i}^{min} \leq Q_{C_i} \leq Q_{C_i}^{max}, \quad i = 1 \ldots\ldots.., N_{QC} \tag{7}$$

The load bus voltage constraints and the maximum value of loadability capacity of the transmission line are,

$$V_{L_i}^{min} \leq V_{L_i} \leq V_{L_{ii}}^{max}, i = 1, \ldots\ldots\ldots, N_{V_L} \tag{8}$$
$$S_{L_i} \leq S_{L_{ii}}^{max}, i = 1, \ldots\ldots\ldots, N_{S_l} \tag{9}$$

where NG defines the number of generators, including the slack bus. N_T, N_{QC}, N_{V_L} and N_{S_l} are the number tap changer transformers, shunt VAR compensators, load buses and transmission lines respectively.

3) PRACTICAL CONSTRAINTS

a: PROHIBITED ZONES OF THE POWER SYSTEM

Three-phase synchronous generators are subject to physical and structural limitations due to failures in shaft bearings and vibrations of machines' accessories such as pumps or boilers. These generators may not operate at certain operating points or regions known as Prohibited Operating Zones (POZ). The concept of POZ was introduced in power system analysis to avoid instability points or zones. The production cost function needs revision to include these prohibited operating zones [81]. Therefore, it is necessary to determine a mathematical formulation for prohibited zones. The POZ constraint for the quadratic fuel cost function is described in Eq. (10) and illustrated in Fig. 1a.

$$\begin{cases} P_{Gi}^{min} \leq P_{Gi} \leq P_{Gi,1}^{lb} \\ or\ P_{Gi,j-1}^{ub} \leq P_{Gi} \leq P_{Gi,j}^{lb} \quad i=1, \ldots, N_G, j=2, \ldots, N_{POZi} \\ or P_{Gi,N_{POZi}}^{ub} \leq P_{Gi} \leq P_{Gi}^{max}, \end{cases} \tag{10}$$

where N_{POZi} is the total number of POZs of generator i; $P_{Gi,j}^{lb}$ and where $P_{Gi,j}^{ub}$ are lower and upper boundaries of the jth POZ of generator i; $P_{Gi}^{\min}$ and $P_{Gi}^{\max}$ are lower and upper limits of active power output of generator i.

b: RAMP-RATE LIMITS

The power output of a generating unit can be increased or decreased in accordance with the limits of the ramp rate, which are a function of the size of the resource. A sudden change in load will affect the generation output. This constraint can be modelled as follows:

$$max\left(P_{G_i}^{min}, P_i^0 - DR_i\right) \leqslant P_{G_i} \leqslant min\left(P_{G_i}^{max}, P_i^0 + UR_i\right) \tag{11}$$

where, P_i^0 is the power generation of the i th unit in the previous hour. DR_i and UR_i are the respective decreasing and increasing ramp-rate limits of the i th unit.

B. OBJECTIVE FUNCTIONS

This study aims to optimize the power system control parameters using the proposed HFO-1 method to minimize the objective functions such as base fuel cost, multi-fuel cost, impact of valve point on fuel cost, power loss, voltage deviation, and fuel cost in POZs. The study utilizes various objective functions listed below.

1) GENERATION FUEL COST MINIMIZATION

a: BASIC FUEL COST

The fuel costs regarding each generator unit are modelled by quadratic functions as:

$$f_C = \sum_{i=1}^{Ng} a_i + b_i P_{Gi} + c_i P_{Gi}^2 \tag{12}$$

where N_g is the total generator number; P_{Gi} is the generation of real power at bus i; a_i, b_i, and c_i are the weighting factors of the generating unit i.

As in (13), shown at the bottom of the next page, a_{ikm}, b_{ikm}, $c_{ikm}$are generator coefficients, and P_{Gikm} is the ith generator active power levels, where i is the generator number, k is the fuel type number, m is the different range of generator levels. P_{Gik} then corresponds to the active power output of Generator i. running on type k. fuel.

b: MULTI FUEL COST

For the case of thermal generating units using multiple fuel options (MFO), a piecewise function is the presentation of fuel cost. Piece wise quadratic equation is used instead of

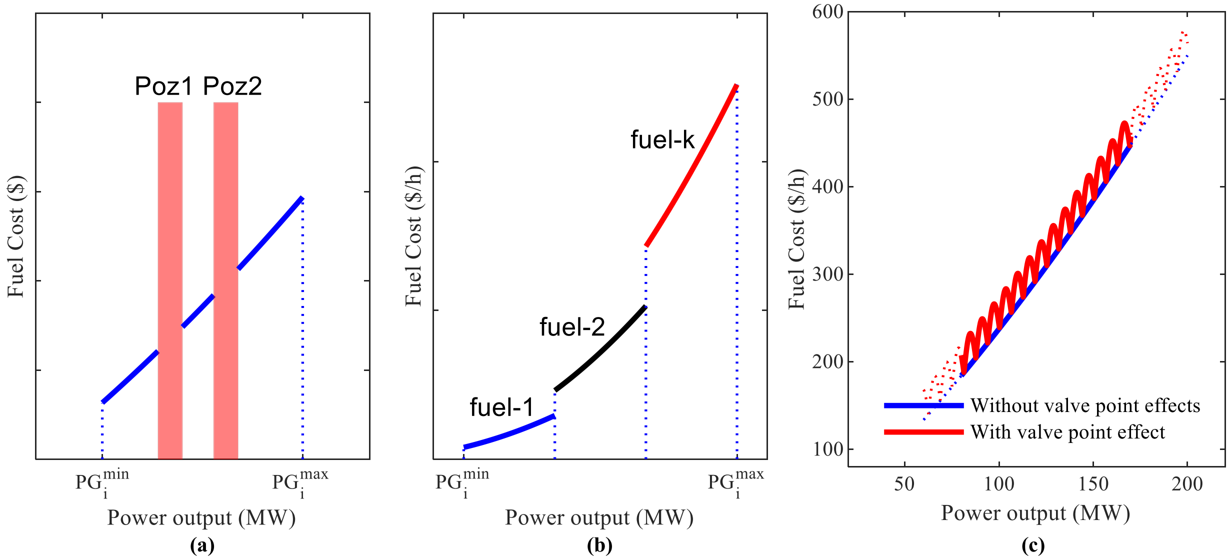

FIGURE 1. The cost graphs (a) curve with prohibited zones, (b) curve multi-fuel cost, and (c) Cost curve with and without the valve-point effect.

normal quadratic equation. The active power levels of generators are considered to have a set of constraints as formulated in (13). They consist of several convex curves as a piecewise sum of quadratic functions, as shown in Fig. 1(b).

c: GENERATION FUEL COST WITH VALVE POINT EFFECT OPTIMIZATION

The fuel cost functions of some generation units are either smooth (without valve point effect) or non-uniform (with valve point effect), as shown in Fig. 1.c. This is due to the fluctuations caused by the opening process of the control valves of the steam turbines. Therefore, taking into account the valve-loading point effect, the fuel cost can be calculated using (14) [81].

$$f_{VC} = \sum_{i=1}^{N_g} \left(a_i P_{gi}^2 + b_i P_{gi} + c_i\right) + \left| d_i \times sin\left(e_i \times \left(P_{gi}^{min} - P_{gi}\right)\right)\right| \quad (14)$$

where d_i and e_i are constants from the valve-point effect of the i^{th} generating unit.

2) TOTAL POWER LOSS

The control parameters are optimized to reduce the real power loss to a minimum. The real power losses for each transmission line can be expressed as,

$$f_{PL} = \sum_{i=1}^{N_L} g_i \left[V_k^2 + V_m^2 - 2V_k V_m cos\left(\delta_k - \delta_m\right)\right] \quad (15)$$

where N_L is the number of transmission lines; g_i is the conductance of the ith line; V_k and V_m are the voltage magnitude at the end buses k and m of the ith line, respectively, and δ_k and δ_m are the voltage phase angle at the end buses k and m.

3) VOLTAGE DEVIATION

In order to improve the voltage profile of the system, the voltage values of all load buses at 1 p.u should be fixed

$$f_{Multi-C} = \begin{cases} \begin{cases} a_{i11} + b_{i11}P_{Gi1} + c_{i11}P_{Gi1}^2, & 1, fuel & P_{Gi11}^{min} \le P_{Gi1} \le P_{Gi11} \\ a_{i12} + b_{i12}P_{Gi1} + c_{i12}P_{Gi1}^2, & 1, fuel & P_{Gi11} \le P_{Gi1} \le P_{Gi12} \\ \ldots & \ldots & \ldots \\ a_{i1\,m} + b_{i1\,m}P_{Gi1} + c_{i1\,m}P_{Gi1}^2, & 1, fuel & P_{Gi1\,m-1} \le P_{Gi1} \le P_{Gi1\,m}^{max} \end{cases} \\ \begin{cases} a_{i21} + b_{i21}P_{Gi2} + c_{i21}P_{Gi2}^2, & 2, fuel & P_{Gi2}^{min} \le P_{Gi2} \le P_{Gi21} \\ a_{i22} + b_{i22}P_{Gi2} + c_{i22}P_{Gi2}^2, & 2, fuel & P_{Gi21} \le P_{Gi2} \le P_{Gi22} \\ \ldots & \ldots & \ldots \\ a_{i2\,m} + b_{i2\,m}P_{Gi2} + c_{i2\,m}P_{Gi2}^2, & 2, fuel & P_{Gi2\,m-1} \le P_{Gi2} \le P_{Gi2\,m}^{max} \end{cases} \\ \begin{cases} \vdots & \vdots & \vdots \\ a_{ik1} + b_{ik1}P_{Gik} + c_{ik1}P_{Gik}^2, & k, fuel & P_{Gik1}^{min} \le P_{Gik} \le P_{Gik1} \\ a_{ik2} + b_{ik2}P_{Gik} + c_{ik2}P_{Gik}^2, & k, fuel & P_{Gik1} \le P_{Gik} \le P_{Gik2} \\ a_{ikm} + b_{ikm}P_{Gik} + c_{ikm}P_{Gik}^2, & k, fuel & P_{Gikm-1} \le P_{Gik} \le P_{Gikm}^{max} \end{cases} \end{cases} \quad (13)$$

HFO-1 Skeleton

1- *Sources* ← initialize_honey_sources
2- *Gbest* ← *Pbest* ←*Sources*[1]
3- **repeat**
4- **for each** *sourceof workers*
5- *component* ← *source*
6- *Sources* ← exploit(*source*, *component*)
7- **for each** *onlooker*
8- *source*← select_a_source(*Sources*)
9- *Sources* ← exploit(*source*)
10- **if** mixing phase
11- *Sources*← mix honey-forms with *PBest* and others randomly
12- ensure the *Pbest* form is not corrupted
13- **if** maturation phase
14- *Sources*← initialize_honey_sources and set *newSite* = *true*
15- **else if** saturation phase
16- *Sources* [*mx*] ← *Pbest* ← Gbest with random *mx* and set *newSite* = *false*
17- **if** *Gbest* is not improved for one maturation period
18- change mixing sizes randomly
19- **until** maximumiteration

by minimizing the voltage deviation [91]. To calculate the voltage deviation for load buses, use the following formula:

$$f_{VD} = \sum_{i=1}^{N_{Pq}} |V_i - 1| \tag{16}$$

where N_{PQ} is the load bus number.

III. HFO-1 ALGORITHM

HFO-1 (Honey Formation Optimization for Single Component) is a swarm-based optimization algorithm that imitates the honey production processes of the bees, and it was introduced by Yetgin and Ercan [90]. It is an extension to the HFO Framework [92] to solve the numerical function optimization problems where the definition of the objective function is not required, and the objective function is used as a black-box interface. The HFO-1 passes through five phases, namely initialization, honey formation, mixing, maturation, and saturation. The skeleton of the HFO-1 algorithm is shown in Scheme 1.

In the initialization phase, the algorithm generates a set of candidate solutions, uniformly random in solution space, corresponding to the bee stoma's initial honey-forms. HFO-1 assumes that every source has its associated honey-form. During the honey formation phase, as the sources are exploited, the initial heterogeneous forms evolve into more mature forms in the bee stoma. In this phase, each honey bee mixes the visited foods with its own enzymes in its stoma and matures its personal mixture overtime. The personal mixture occurring in the bee stoma is simply called mixing-0 and modeled with the exploit function in the algorithm, defined through (17)-(19). Let $x_i = Sources_i$ denotes the i. solution among N solutions, $x_i.f = f(x_i)$ is its honey fitness (objective value), $x_i.c = f(x_i) - Gbest.f$ is its component fitness, Gand best is the global best solution of the previous iteration. Then, the candidate solution v_i is generated around the solution x_i and then the solution is updated if the v_i has a better component for workers or better honey fitness for onlookers, defined in (18) and (19) respectively.

$$v_i[j] = x_i[j] + q.\,(x_i[j] - x_k[j]) \tag{17}$$

$$Sources_i = \begin{Bmatrix} v_i, & if\ v_i.c < x_i.c \\ x_i, & otherwise \end{Bmatrix} \tag{18}$$

$$Sources_i = \begin{Bmatrix} v_i, & if\ v_i.f < x_i.f \\ x_i, & otherwise \end{Bmatrix} \tag{19}$$

where $x_k \neq x_i$ is a random source and j is the randomly selected dimensions to update (the length of j is strategic and defined in the original paper), and q is the step size. Also, each worker i select the source i whereas each onlooker selects a source i according to the roulette selection strategy (22) whose selection probability vector $P = [p_1, p_2, \ldots, p_N]$ is defined through (20)-(21) where p_i is the probability of the selection of the source i, Sources.f is the vector of all objective values of the solutions, RouletteWheelSelection(P) selects one index according to P.

$$fit_i = \frac{1}{x_i.f - min(Sources.f) + 0.001} \tag{20}$$

$$p_i = \frac{fit_i}{\sum_{k=1}^{N} fit_k} \tag{21}$$

$$i = RouletteWheelSelection(P) \tag{22}$$

When the honey-form in the bee stoma is matured enough the bees mix their personal mixtures among themselves in the hive by sharing via mixing sessions, which occurs in the mixing phase. This phase corresponds to chewing and spitting cycles of the honey-forms from one mouth to the other. The algorithm assumes two types of mixing in the hive: mixing-1 and mixing-2, for mixing semi-mature and mature forms, respectively. In both cases, the solution update occurs according to (23) where a random portion of a solution, either a random solution x_k or Pbest (population best of the previous iteration), defined by the index vector jk, is transferred to a random portion of x_i, defined by the index vector j.

$$x_i[j] = \begin{Bmatrix} x_k\,[jk], & if\ rand > 0.5 \\ Pbest[jk], & else \end{Bmatrix} \tag{23}$$

Both vectors, j and jk, have the same length, which is strategically selected and defined as the mixing size in the original algorithm. Also, note that the mixing size is randomly acquired and adaptively tuned by the algorithm when the Gbest is not changed for one period, shown in steps 17-18 of the algorithm. During the maturation phase, the honey-forms become homogenous, meaning the same as the Pbest in an epsilon neighborhood. This phase occurs when the bees fully exploit the current site, and the honey production must continue from a new site. This phase continues as long as the Gbest does not change until the time that the bees must finalize the honey production, which is the saturation phase. In this phase, the Gbest gradually metamorphoses the mixture to speed up the homogeneity of the mixture. You can find detailed information about the HFO-1 algorithm in the study conducted by Yetgin and Ercan [90].

A. HFO-1 MODIFICATION-A (HFO-1A)

HFO-1 was originally designed for numerical optimization problems where all the problem dimensions are considered to have the same search range for simplicity. However, many real-life optimization problems have different search ranges for various dimensions, and this may create possible violating bounds in the mixing phase due to mixing different dimensions of the solutions at (23). Thus, (24) is proposed to be added to the end of mixing phase to correct any possible violating bounds at (23). This approach also adds new behaviour in mixing phase to increase the exploration ability of the algorithm. Thus, if any violating bounds exist, those dimensions of the solution are randomly generated from their corresponding search ranges, and this may contribute to the ability of the bees to explore.

$$x_i[j_k] = \left\{ \begin{array}{l} rand\left(low_{j_k}, up_{j_k}\right), \ if \ x_i[j_k] > up_{j_k} \\ rand\left(low_{j_k}, up_{j_k}\right), \ if \ x_i[j_k] < low_{j_k} \end{array} \right\} \tag{24}$$

where j is the vector of selected dimensions to update, acquired in (23), j_k is the k. component of the vector j violating the limits, low and up are the lower and upper bounds as vectors.

B. HFO-1 MODIFICATION-B (HFO-1b)

In order to control the possible violating bounds in the mixing phase, another solution is to change the mixing phase itself in such a way that violating the bounds is avoided in advance. (25) is proposed to replace (23) to change the mixing behavior of the bees to ensure the limits.

$$x_i[j] = \left\{ \begin{array}{ll} 0.5 * (x_m[j] + x_n[j]), & if \ rand > 0.5 \\ 0.5 * (x_m[j] + Pbest[j]), & else \end{array} \right\} \tag{25}$$

where j is the vector of selected dimensions to update, $x_m \neq x_i$ and $x_n \neq x_i$ are randomly selected sources to mix from.

C. HFO-1 MODIFICATION-C (HFO-1c)

HFO-1 Modification-C is an extension to the Modification-A. Here, different solution update equations are proposed for workers (26) and onlookers (27). In the solution update equation of HFO-1 (17), the solutions, x_i and x_k, might already be modified in the current generation. A different approach is proposed in (26)-(27) where the solutions at the right side of the equation (e.g., px_i and others) are not allowed to be modified in the current generation, and also, x_k in the original equation is replaced by strategic selections, permutation ($permx$) and roulette selections (px_{sel}). This approach also allows vectored implementation, which is not possible in the original. In order to achieve this, $letpSources = Sources$ be the population before its update, and $permx = shuffle(pSources)$ be its randomly reordered (permutated) variant, $px_i = pSources_i$ and $px_{sel} = pSources_{sel}$ where the sel is the selected index by the onlooker according to the selection strategy, defined through (28)-(29) where p_i is the i. element of the probability vector P. Then, the population $Sources$ is updated based on the component fitness for workers (30) and honey fitness for the onlookers (31).

$$v_i[j] = px_i[j] + q.\left(px_i[j] - permx_i[j]\right) \tag{26}$$

$$v_i[j] = px_i[j] + q.\left(px_i[j] - px_{sel}[j]\right) \tag{27}$$

$$p_i = 0.1 + 0.9 * \frac{fit_i}{\sum_{k=1}^{N} fit_k} \tag{28}$$

$$sel = RouletteWheelSelection(P) \tag{29}$$

$$Sources_i = \left\{ \begin{array}{ll} v_i, \ if \ v_i.c < px_i.c \\ x_i, \quad otherwise \end{array} \right\} \tag{30}$$

$$Sources_i = \left\{ \begin{array}{ll} v_i, \ if \ v_i.f < px_i.f \\ x_i, \quad otherwise \end{array} \right\} \tag{31}$$

Note that in this modification, similar to workers, each onlooker is also associated with a different source (each onlooker i select the source i). However, each onlooker applies roulette selection to mix one step from a random source, px_{sel}.

D. ADAPTATION OF PROPOSED HFO-1 ALGORITHM FOR POWER FLOW CONSTRAINTS

In this study, HFO-1 is adapted to overcome undesirable solutions by adding a penalty value to the objective function when solving the OPF problem with constraints. Thus, the algorithm assumes bound constraints such that real power generation output at the slack bus (P_{Gslack}), load bus voltages (V_L), reactive power generation output (Q_G) and transmission line loading (S_{TL}) are included in the extended objective function to ensure that the dependent variables remain within the allowed limits and to discard any infeasible solution. Let $u = \left[P_G \ V_G \ Q_C \ T\right]$ denote any solution vector and $x = [P_{Gslack} Y]$ with $Y = [V_L Q_G S_{TL}]$ denotes the vector of constraint parameters. Then, the objective function value, $f(x)$, is updated by sequential operations via (32)-(35) to penalize any violating boundary. If the slack variable violates the bounds, it is penalized with a weight of 1000 as shown in (33).

$$[P_{Glsack}, Y] = PowerFlow(u) \tag{32}$$

$$\begin{aligned} P_{Glsack} = {} & 1000.P_{Glsack} \\ & \times .(P_{Glsack} > Ub_{Glsack} || P_{Glsack} < Lb_{Glsack}) \end{aligned} \tag{33}$$

$$\begin{aligned} Penalty(Y) = w.\sum\nolimits_{i=1}^{n} & [abs(Ub_i - Y_i).(Y_i > Ub_i) \\ & + abs(Lb_i - Y_i).(Y_i < Lb_i)] \end{aligned} \tag{34}$$

where $PowerFlow(x)$ function is defined according to [93], Ub_{Glsack} and Lb_{Glsack} are upper and lower bounds of the slack variable respectively, Ub_i and Lb_i are upper and lower bounds of the i. constraint parameters respectively, w is the penalty coefficient and empirically found for each multi-objective function definition. Then, the objective function value, $f(x)$, used in the algorithm is updated by (35) where the objective function uses the slack variable as defined in (33) (if in case) and adds a further penalty to any violating bounds.

$$f(x) = f(x) + Penalty(Y) \tag{35}$$

In addition, the procedure for taking the POZ into account can be explained as follows: When a generator operates within the POZ, the strategy is to add a penalty value to the total objective function. This penalty term is based on the distance of the operating point from the lower or upper band of the POZ.

IV. BENCHMARK RESULTS AND OPF CASE STUDIES

This section is organized as follows. First, 12 benchmark functions are tested to measure the performance of the three proposed variants of HFO-1, and the numerical results are given in the first subsection. Then, in the second subsection, IEEE-30 and IEEE-118 busbar test systems are used to verify the effectiveness of the proposed variants, and their results are evaluated.

A. BENCHMARK RESULTS OF PROPOSED HFO-1 MODIFICATIONS

To verify the effectiveness of the proposed variants of HFO-1 in different problems, they are comparatively tested using the CEC 2021 benchmark functions. CEC 2021 Test Suite includes 12 unimodal, multimodal, hybrid and composite functions. Each benchmark function is experimented with 30 times, with a maximum iteration of 5000, and the results are averaged. The population size 30 is used, which is equal to the number of food sources, and the problem dimension 10 is used for all functions. Each function's search range is fixed as [−100,100]. Thus, for the benchmark tests, HFO-1a is equivalent to the original HFO-1 due to the fact that HFO-1a only differs from HFO-1 when the search range is different for some dimensions. The suggested parameter values of HFO-1 are used, which assumes that the mixing ratio (MR) is 8, the initial step size(q0) is 2, and random walk-based search is enabled. The purpose of this test is to comprehensively investigate the overall performance of the proposed algorithms to better demonstrate their effectiveness and ability to solve other complex optimization problems. Table 1 shows the results for the best, worst, average, and execution time of the 12 benchmark functions, with the best results in bold.

The variants of the HFO-1 are very successful in finding the optimum solution for unimodal functions such as F1, F2, F3, F4, F5, F7, and F11, as shown in Table 1. However, as a general established knowledge from literature, no optimization algorithm is expected to overcome the others for all test functions. For example, HFO-1a shows superior success for the challenging function, such as F9 whereas other variants of HFO-1 get better optimum values for the functions F6, F8, and F10. Here the variants of HFO-1 are compared among themselves in terms of the average values obtained after 30 iterations. Talking in general, the HFO-1c algorithm seems superior to the others in terms of execution time and optimum values, whereas HFO-1b seems the worst in terms of the same metrics for the benchmark problems. The reason is that HFO-1c allows vectorial implementation, which makes it faster than the others for the test problems. The solution update equations (25)-(26) of HFO-1c allow each bee to behave more independently. This helps HFO-1c to escape from the local optimums at which the other variants are possibly get stuck.

Fig. 2 visualizes the first 1000 iterations of the evolution curves of the HFO-1 variants for the CEC 2021 benchmark test functions. This may give a general picture of their convergence rates. Comparing HFO-1a, which is used here as the original HFO-1, with the other variants (HFO-1b and HFO-1c), the convergence rates of the algorithms seem more or less similar. However, the convergence rates of the improved algorithms are slightly better than the original one, except for F1. Talking in general, the HFO-1c variant seems the best when considering its optimization accuracy and convergence rate, which makes it potentially an effective optimization algorithm to address a growing number of problems.

Fig. 3 shows the boxplot curves of the variants of HFO-1. The figure visually represents the data distribution across all functions in the CEC 2021 dataset. The whiskers on the boxplots represent the minimum and maximum values obtained by the algorithms. A tight boxplot is indicative of a significant level of data reconciliation, as is the case for functions such as F1, F2, F3, F5, F7, F9, F10, and F11 of variants of HFO-1. Apart from these, HFO-1c also has a tight box plot in F8 and F12. When the functions F4 and F6 are analyzed, HFO-1c gives a more stable result than HFO-1a and HFO-1b.

B. OPF CASE STUDIES

To assess the effectiveness of our proposed algorithms, we utilized the OPF problem to solve the IEEE 30 and 118 bus systems. eleven test cases are configured. Each test case is experimented with the proposed algorithms, each of which uses a population size of 30 and a maximum iteration of 10,000. The problem dimension is decided by the bus system considered. The suggested parameter values of the HFO-1 are followed, which assumes MF = 8, qo = 2, and random walk enabled.

Table 2 presents the data, specifications, and minimum and maximum operating constraints for both test systems. Further details can be found in references [82], [83]. It is applied the penalty technique to ensure that both test systems and control variables, including valve point effect, multi-fuel operation, and POZs, remained within the acceptable ranges specified in Table 2. 11 case and two sub-case studies were examined across IEEE test systems, as summarized in Table 3. A tick mark has been placed in the Table 3 for the specified case studies. To demonstrate the effectiveness of HFO-1 variants in solving the OPF problem, we compare them with several algorithms reported in the literature. Graphical comparisons are also presented to investigate the convergence performance

TABLE 1. The statistical comparison of the HFO-1 variants for the CEC 2021 benchmark functions.

Functions		HFO-1a	HFO-1b	HFO-1c
F1	Best	300	300	300
	Worst	300	300	300
	Average	**300**	**300**	**300**
	Time	2.18791886333	3.02335361000	0.20209477000
F2	Best	400	400	400
	Worst	400	400	400
	Average	**400**	**400**	**400**
	Time	17.9947113300	27.1486671666	0.34738551666
F3	Best	600	600	600
	Worst	600	600	600
	Average	**600**	**600**	**600**
	Time	5.11515254666	5.00776979000	0.53332531333
F4	Best	800	800	800
	Worst	802.984877171	802.984877171	802.984877171
	Average	801.392946779	801.193950868	**801.094454969**
	Time	83.3045264933	83.5998533833	13.3312779733
F5	Best	900	900	900
	Worst	900	900	900
	Average	**900**	**900**	**900**
	Time	4.06213926000	5.73868752000	0.14919569666
F6	Best	1800.02028520	1800.00289384	1800.00095751
	Worst	1800.96374800	1803.01264169	1800.09834707
	Average	1800.10867943	1800.18825223	**1800.03196080**
	Time	81.5295195033	81.5953919800	19.3705893200
F7	Best	2000	2000	2000
	Worst	2000	2019.99986136	2000
	Average	**2000**	2000.66666204	**2000**
	Time	13.1520806466	19.2498914966	29.1754165566
F8	Best	2200.00000651	2200.00000234	2200.00044175
	Worst	2200.72303619	2220.03817503	2200.05576148
	Average	2200.26700857	2202.11578475	**2200.00645231**
	Time	528.516453223	91.3621118900	33.9798624466
F9	Best	2300	2529.28438270	2529.28438270
	Worst	2529.28438270	2529.28438270	2529.28438270
	Average	**2521.64156995**	2529.28438270	2529.28438270
	Time	82.8267290400	83.7399328533	30.7012996600
F10	Best	2500.06039397	2500.00905952	2400.00000000
	Worst	2500.21065977	2500.20565234	2500.20804879
	Average	2500.13850257	2500.08339698	**2490.13976509**
	Time	82.7537711233	83.5873239133	28.1563702100
F11	Best	2600	2600	2600
	Worst	2600	2600	2600
	Average	**2600**	**2600**	**2600**
	Time	5.73114099666	6.10654728666	3.29754288333
F12	Best	2858.61835455	2858.61835455	2858.61835455
	Worst	2858.61835455	2861.43526767	2858.61835455
	Average	**2858.61835455**	2859.01107171	**2858.61835455**
	Time	125.868053160	827.455811576	39.497679126

of HFO-1a, HFO-1b, and HFO-1c. The results show that all constraints are strictly adhered to the acceptable ranges when the algorithms start converging. The figures only show the penalty curve of the best variant, which becomes zero when all constraints are satisfied

1) IEEE 30-BUS SYSTEM

The system demand for active power was 2.834 p.u and for reactive power was 1.262 p.u at 100 MVA base. The system includes six generators, four transformers with off-nominal tap ratios at lines 6-9, 6-10, 4-12, and 28-27, and two shunt compensators for standard system and nine shunt compensators modified system. The effect of practical constraints was examined by conducting 2 case studies in the standard test system. A seven-case study was conducted by integrating renewable energy sources in the modified test system. The load demands are modeled as fixed loads from the literature. The coefficients for the fuel cost are available in [94].

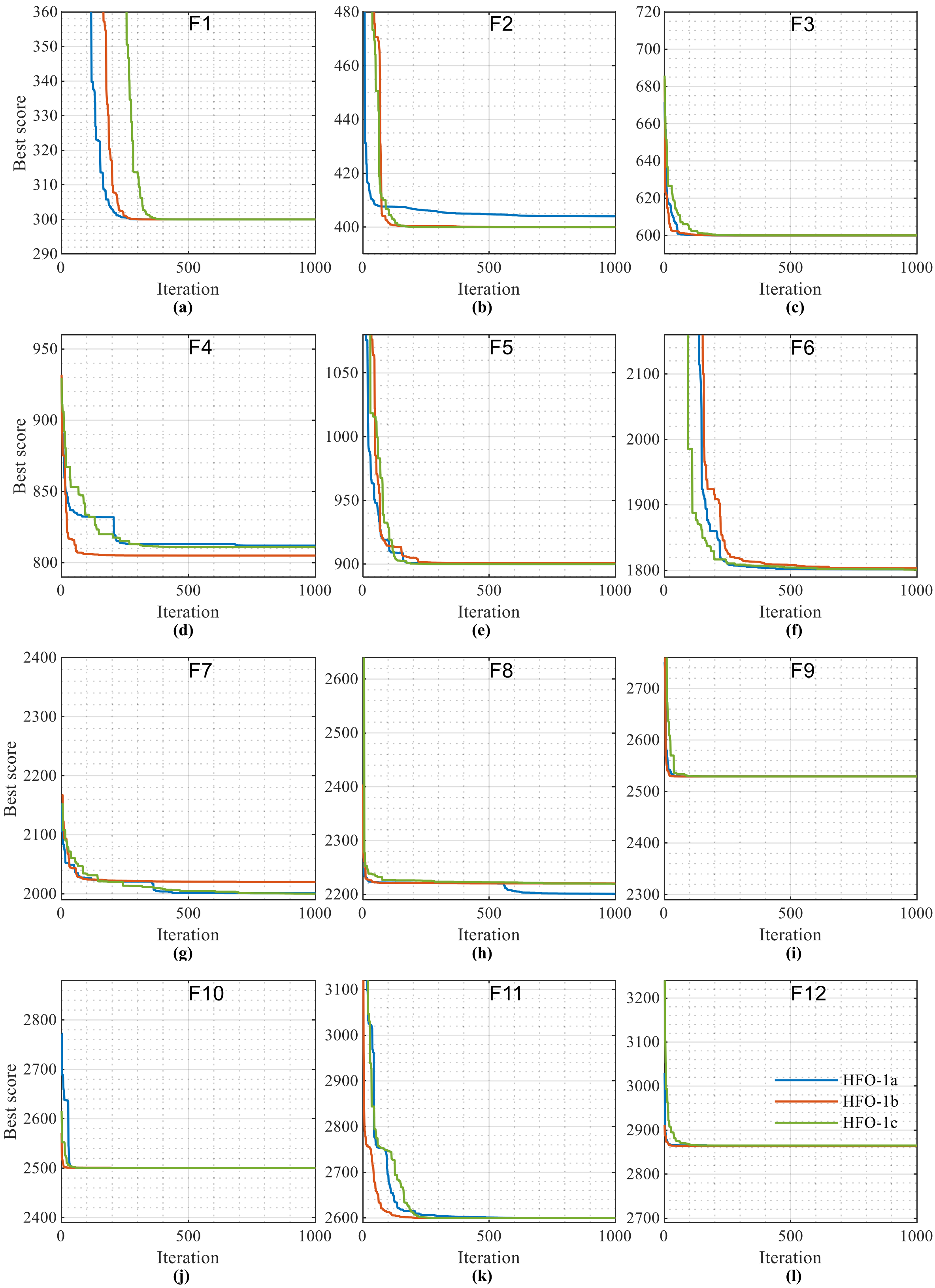

FIGURE 2. Benchmark converge curve graphs for CEC 2021 twelve functions (a)-(l).

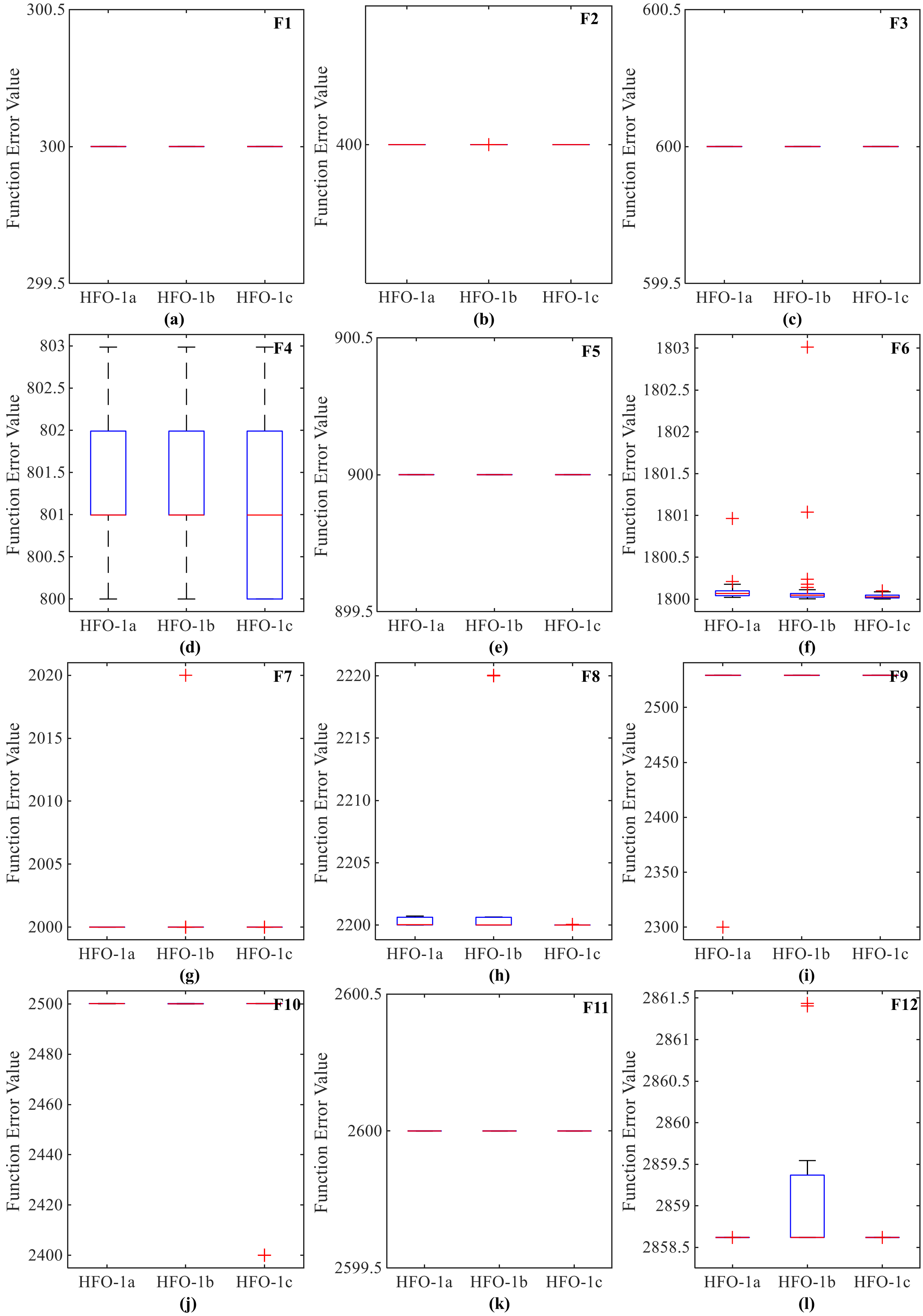

FIGURE 3. Boxplot graphs for CEC 2021 twelve functions (a)-(l).

a: THE STANDARD SYSTEM

There are eighteen control variables for this system. In case no 1, fuel cost is minimized without practical constraints. In case 2, active power loss is minimized both with and without ramp-rate limits.

TABLE 2. IEEE 30 and 118 bus test system.

	IEEE 30 Bus Test System			IEEE 118 Bus Test System		
Items	Quantity	Description	Range	Quantity	Description	Range
Buses	30	[82]		118	[83]	
Branches	41	[83]		186	[83]	
Generators	6	Buses:1(Slack),2,5,8,11,13 V_G [pu]	[0.95 1.1]	54	Buses:1,4,6,8,10,12,15,18,19,24,25,26,27,31,32,34,36,40,42,46,49,54,55,56,59,61,62,65,66,69(Slack),70,72,73,74,76,77,80,85,87,89,90,91,92,99,100,103,104,105,107,110,111,112,113,116	[0.94 1.06]
Shunt capacitors	9	*Standard system*		14	Buses:18,25,53	[0 30]
		Buses:10,12,15,17,20,21,23,24,29	[0.0 5 .0]			
	2	*Modified system*				
		Buses:10,24	[0 30]			
Transformers	4	Buses:11, 12, 15, 36 T [pu]	[0.95 1.1]	9	Buses:8,32,36,51,93,95,102,107,127	[0.95 1.1]
Load buses	24	Voltages V_L [pu]	[0.95 1.05]	64	Voltages V_L [pu]	[0.94 1.06]
Control variables	17	Standard system		130		
	24	Modified system				
	11	Modified integrated renewable system				

TABLE 3. Summary of case studies on test systems.

	IEEE 30-bus									IEEE 118-bus	
Case no.	Standard system		Modified system						Renewable system	Standard system	
	f_C	f_{PL}	f_C	f_{PL}	f_{VD}	$f_{\text{Multi-C}}$	f_{VC}	f_{POZ-C}	f_C	f_C	f_{PL}
Case 1	✓										
Case 2.1 (without ramp rate and POZ)		✓									
Case 2.2 (wit ramp rate and POZ limit)		✓									
Case 3			✓								
Case 4				✓							
Case 5					✓						
Case 6						✓					
Case 7							✓				
Case 8								✓			
Case 9									✓		
Case 10										✓	
Case 11											✓

In the first case study, where (12) was used to minimize the basic fuel cost, the fuel cost of HFO-1c and HFO-1b were found to be 800.59727 $/h and 800.597793 $/h, respectively. On the other hand, the fuel cost of HFO-1a was 800.597226 $/h.

Fig. 4 displays the convergence curves of the three developed HFO-1 modifications and the penalty value of the best-performing HFO-1 variant. The penalty plot on the right-hand side of Fig. 4-11 belongs to the HFO-1 modifications, which provides the optimal solution value for each

TABLE 4. Simulation results of case 1 on IEEE-30 bus standard test system for practical system.

		Existing methods						*Proposed*		
Items	Range	TS [96]	PSO [97]	CSA [97]	HCSA[97]	HFFA [97]	UDTPSO [95]	HFO-1a	HFO-1b	HFO-1c
P_1	[80 250]	176.04	178.5558	170.7789	176.8707	179.3122	177.7624	177.1952	177.1937	177.1960
P_2	[20 80]	48.76	48.6032	48.3696	49.88626	48.26495	48.9829	48.72334	48.72260	48.72369
P_5	[1550]	21.56	21.6697	18.3135	21.61352	20.9265	21.0188	21.38353	21.38337	21.38335
P_8	[1035]	22.05	20.7414	32.6057	20.87963	19.86292	21.02163	21.23662	21.23427	21.23680
P_{11}	[10 30]	12.44	11.7702	10	11.61685	12.3402	11.43384	11.91973	11.92443	11.91860
P_{13}	[12 40]	12	12	12	12	12	12	12.00000	12	12.00000
V_1	[0.95 1.1]	1.0500	1.1	1.1	1.057	1.1	1.1	1.083319	1.083328	1.083308
V_2	[0.95 1.1]	1.0389	0.9	1.0567	1.045622	1.057657	1.087706	1.024304	1.044312	1.024294
V_5	[0.95 1.1]	1.0110	0.9642	1.0912	1.018493	1.065718	1.061636	1.033132	1.033142	1.033126
V_8	[0.95 1.1]	1.0198	0.9887	1.0725	1.026591	1.070609	1.069037	1.057877	1.047877	1.057874
V_{11}	[0.95 1.1]	1.0941	0.9403	1.0465	1.057	1.025229	1.007715	1.099991	1.063684	1.099999
V_{13}	[0.95 1.1]	1.0898	0.9284	1.1	1.057	1.092478	1.099918	1.053197	1.053168	1.053247
$Q_{c\text{-}10}$	[0 5.0]	-	9.0931	30	25.35913	5	19.49261	1.599661	14.78210	1.578098
$Q_{c\text{-}24}$	[0 5.0]	-	21.665	6.7556	10.6424	29.67086	15.07354	11.13993	11.13698	11.13735
T_{11}	[0.9 1.1]	1.0407	0.9848	1.0531	1.025462	1.045322	0.97872	1.034924	1.026793	1.034890
T_{12}	[0.9 1.1]	0.9218	1.0299	1.007	0.972648	0.980038	0.957272	0.900023	0.926474	0.900000
T_{15}	[0.9 1.1]	1.0098	0.9794	1.0395	1.006042	1.096105	0.99571	0.964433	0.964427	0.964506
T_{16}	[0.9 1.1]	0.9402	1.0406	0.9707	0.964443	1.02131	0.975997	0.966121	0.966117	0.966124
Q_1	[-20 150]	-	-	-	-	-	-	2.656381	2.665909	2.648250
Q_2	[-20 60]	-	-	-	-	-	-	20.24224	20.24073	20.22889
Q_5	[-15 62.5]	-	-	-	-	-	-	25.72783	25.73005	25.73033
Q_8	[-15 48.7]	-	-	-	-	-	-	26.87082	26.84489	26.87458
Q_{11}	[-10 40]	-	-	-	-	-	-	26.80601	11.10547	26.80788
Q_{13}	[-15 44.7]	-	-	-	-	-	-	2.496155	2.474280	2.533501
f_C(\$/h)		802.29	803.4548	802.7283	802.0347	800.9964	799.5376*	**800.5972**	800.5977	800.5972
f_{PL}(MW)		-	9.9403	8.6677	9.466955	-	8.819618	9.058451	9.058483	9.058532
f_{VD} (p.u)		-	-	-	-	-	-	0.889625	0.882227	0.889498

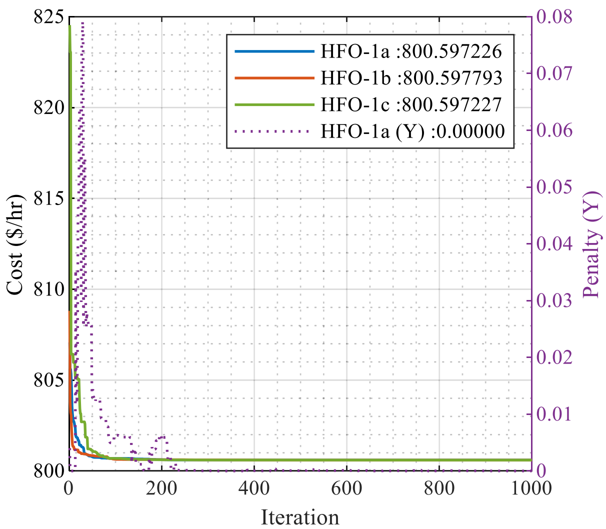

FIGURE 4. Basic fuel cost convergence of HFO-1a, HFO-1b and HFO-1c for without practical constraints for the standard test system.

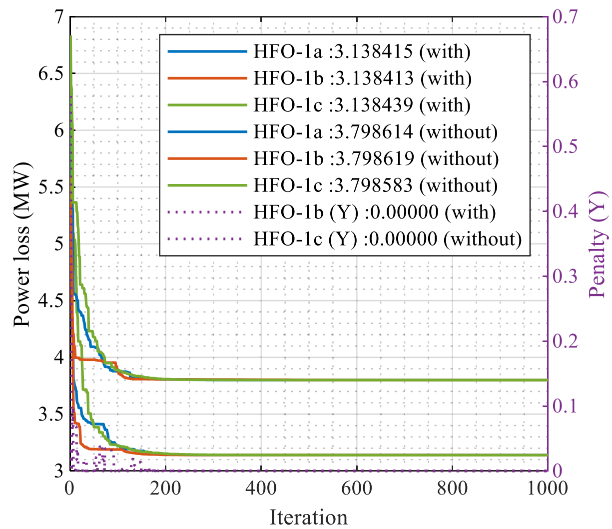

FIGURE 5. Power loss convergence of HFO-1a, HFO-1b and HFO-1c for with and without practical constraints for the standard test system.

case study. In these figures, the penalty value of the best performing HFO-1 variant is plotted for each case study, and it is clearly presented that the safety and operating constraints of the power system are strictly adhered to.

Case 2 contains two subcases: with ramp rate limits and POZ and without ramp-rate limits and POZ. In the first subcase (Case 2.1), HFO-1b converged to a better result than the other variants, and in the second subcase (Case 2.2), where there were no practical restrictions, HFO-1c converged to a better result.

Fig. 5 compares the convergence speed of the best performing variant among the three HFO-1 modifications developed, with and without practical constraints.

HFO-1a and HFO-1b exhibit similar convergence and superiority over the HFO-1c algorithm. Table 4 shows the comparison of the solutions produced by HFO-1 variants with existing methods without practical constraints. In this table, the solutions produced by HFO-1 variants are compared in detail with existing methods. Table 5 gives the results of the study in which the active power loss was minimized without practical constraints and with practical constraints which with ramp rate and POZ limit. It can be seen in both tables that the variants the proposed HFO-1 algorithm yields superior results than existing methods. The ramp –rates and POZ limits followed by the generating units for the objective function can be found from [95]. The practical constraints set for the generators have been observed throughout the simulation.

Upon careful analysis of Table 4, it can be seen that the generators attempt to reduce fuel costs by producing active power as close to the lower limit values as possible. In contrast, as shown in Table 5, the opposite is observed. For the sub-cases with and without practical constraints, all generators except the swing bus generate power at the highest limit value. This is a predictable outcome, as the active power generation of the released swing bus is reduced in order to minimize power loss.

The results were validated with existing literature in the standard test system category and the findings are presented in Table 6.

b: THE MODIFIED SYSTEM

In the first case study for this the system, the fuel cost of HFO-1c was found to be 800.3871 \$/h, and the fuel cost of HFO-1a was 800.3874 \$/h. Fig.6 displays the convergence curves of the three developed HFO-1 modifications and the penalty value of the best-performing HFO-1. Although HFO-1a has a faster convergence speed than the other two variants, HFO-1c outperforms them and achieves the best optimal value.

In case 4, where active power loss is minimized, HFO-1a outperforms HFO-1b and HFO-1c with a value of 3.07626 MW. Fig.7 compares the convergence speed of the three developed HFO-1 modifications. HFO-1a and HFO-1b exhibit similar convergence and superiority over the HFO-1c algorithm. The voltage increase at the load bus is an important factor for OPF. Case study 5 aims to keep the voltages at 1.p.u by utilizing (16). Table7 shows that HFO-1c is 0.08350 p.u, while HFO-1a and HFO-1b are 0.08413 p.u and 0.08403 p.u, respectively. Thus, HFO-1c achieves a much lower voltage deviation value compared to other HFO-1 variants. As clearly seen from Fig. 8, HFO-1c tends to have a softer (slower) convergence. Just like in case 3, it performs extra well in the later iterations and reaches the best result.

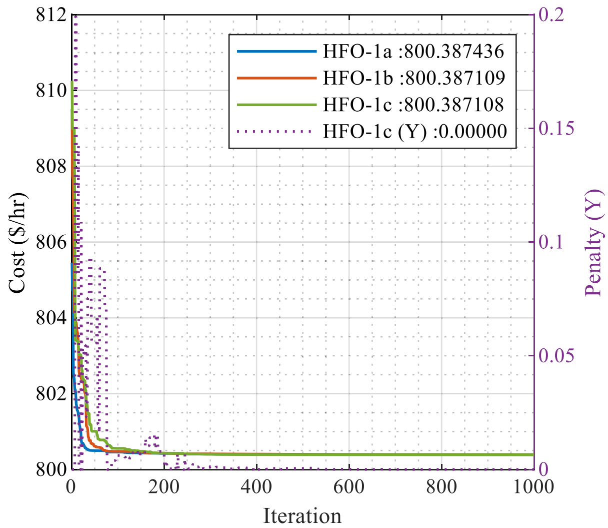

FIGURE 6. Basic fuel cost convergence of HFO-1a, HFO-1b and HFO-1c for the modified test system.

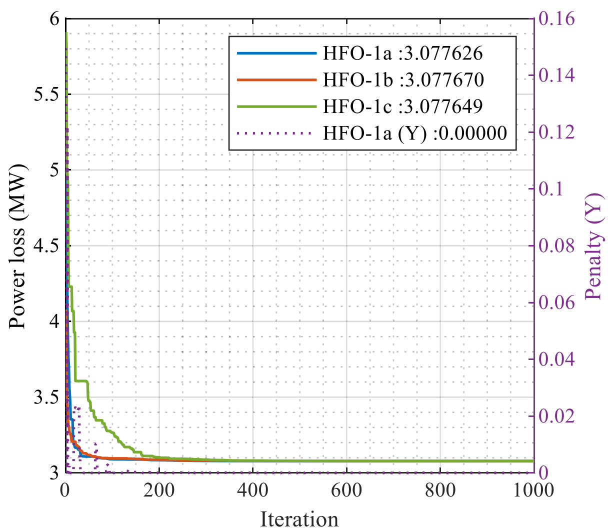

FIGURE 7. Active power loss convergence of HFO-1a, HFO-1b and HFO-1c for the modified test system.

It was aimed to minimize the multi-fuel cost in the 5th case study, which was carried out by carefully optimizing all control parameters and strictly adhering to the safety constraints of the power system. The proposed algorithm's best result was found with sub-variant HFO-1b, which yielded a value of \$646.3758/h. HFO-1b not only outperformed the other modified variants but also demonstrated the fastest convergence in solving this problem, as shown in Fig.9. The seventh case study investigates the fuel cost problem of the sine-function valve effect.

The results obtained are impressive. HFO-1a costs \$823.9815 per hour, while HFO-1b and HFO-1c cost \$823.9813 per hour. Fig.10 shows that the HFO-1b variant outperforms the other two variants in terms of both value and convergence speed. The 8th case study analyzes the

TABLE 5. Results of case 2 on IEEE-30 bus standard test system for with and without practical system.

Items	*Existing methods*				*Proposed*					
	HCSA [97]		UDTPSO [95]		HFO-1a		HFO-1b		HFO-1c	
	without	with	without	with	without	with	without	with	without	with
P_1	51.608	82.521	51.34983	82.12314	51.538415	82.198614	51.53841	82.198619	51.53843	82.19858
P_2	80	63	80	63	80.000000	63.000000	80.00000	63.000000	80.00000	63.00000
P_5	50	49	49.99966	49	50.000000	49.000000	50.00000	49.000000	50.00000	49.00000
P_8	35	30	35	30	35.000000	30.000000	35.00000	30.000000	35.00000	30.00000
P_{11}	30	28	30	28	30.000000	28.000000	30.00000	28.000000	30.00000	28.00000
P_{13}	40	35	40	35	40.000000	35.000000	40.00000	35.000000	40.00000	35.00000
V_1	1.057	1.057	1.1	1.1	1.061488	1.065626	1.061477	1.065673	1.061441	1.065675
V_2	1.0562	1.0037	1.098277	1.026681	1.037422	1.047541	1.037435	1.027582	1.047377	1.037578
V_5	1.0383	1.0324	1.08068	1.077312	1.037951	1.037173	1.037936	1.037195	1.037900	1.037198
V_8	1.0461	1.057	1.08905	1.072681	1.054283	1.042319	1.054239	1.042352	1.044231	1.052356
V_{11}	1.057	1.057	0.996508	1.038465	1.093636	1.093563	1.093433	1.094045	1.093042	1.093978
V_{13}	1.057	0.9308	1.099818	1.1	1.062996	1.062647	1.063122	1.062387	1.063350	1.062385
$Q_{c\text{-}10}$	21.4206	30	28.28745	24.9794	0.000032	0.000861	0.000003	0.000000	0.000004	0.000001
$Q_{c\text{-}24}$	16.5347	16.5028	13.42331	11.96349	11.105200	11.129881	11.09797	11.096061	11.10928	11.11171
T_{11}	1.0134	0.9624	1.010603	0.973144	1.032067	1.029264	1.031877	1.029674	1.031560	1.029581
T_{12}	0.9629	0.9715	0.964953	0.989799	0.900000	0.900012	0.900000	0.900000	0.900000	0.900000
T_{15}	0.9802	0.9	0.994236	0.975125	0.989169	0.987220	0.989365	0.986775	0.989740	0.986791
T_{16}	0.9654	0.9349	0.970434	0.964664	0.969450	0.968308	0.969396	0.968289	0.969427	0.968270
Q_1	-	-	-	-	-5.432830	-4.305339	-5.48436	-4.264374	-5.46741	-4.25276
Q_2	-	-	-	-	7.554060	8.852705	7.644912	8.882740	7.537221	8.865033
Q_5	-	-	-	-	21.744717	21.928257	21.73931	21.906322	21.74894	21.91387
Q_8	-	-	-	-	26.741791	26.794728	26.70693	26.767812	26.77170	26.78868
Q_{11}	-	-	-	-	24.317096	23.887919	24.21729	24.129988	24.02514	24.08723
Q_{13}	-	-	-	-	10.871538	10.368102	10.96790	10.168800	11.14332	10.16669
f_C($/h)	967.9202	913.5794	887.7182	963.4638	1013.09150	27288204.1	1013.090	27288204.1	1013.091	27288204
f_{PL}(MW)	3.208	4.121	3.723141	2.949494	3.138415	3.798614	**3.138413**	3.798619	3.138439	**3.798583**
f_{VD} (p.u)	-	-	-	-	0.885580	0.885544	0.885336	0.885816	0.884861	0.886128

TABLE 6. Validation of simulation results of case studies 1-2 on IEEE-30 bus standard test system.

Methods	Case 1	Case 2	
	without	with	without
EP [98]	803.754		
MSFLA [87]	802.287		
AGSO [99]	801.75		
Hybrid MSFLA-PSO [100]	801.753		
IPSO [26]	801.978	5.0732	
CSA [97]	802.7283		
HCSA [97]	802.0347	4.121	3.208
UDTPSO [95]	799.5376*	3.7231	2.9494
HFO-1a	**800.597226**	3.79861	3.138415
HFO-1b	800.597793	3.79861	**3.138413**
HFO-1c	800.597227	**3.79858**	3.138439

* Since control variables were not provided, it not validated.

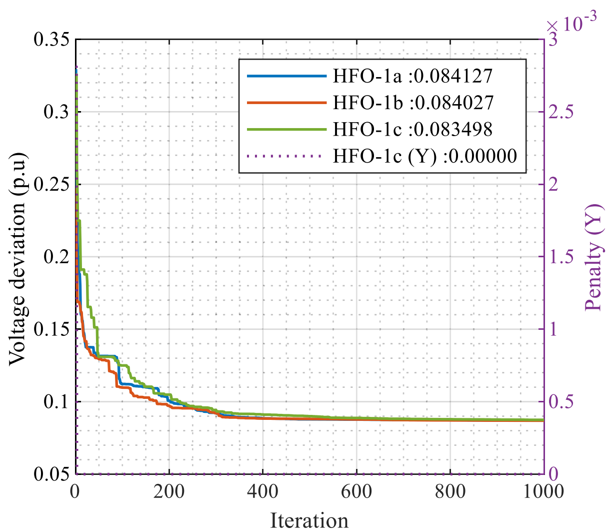

FIGURE 8. Voltage deviation convergence of HFO-1a, HFO-1b and HFO-1c for the modified test system.

issue of generation cost with prohibited operating zones. This problem necessitates an additional constraint on the operation of the generators in addition to the control variable constraint for this test system. All control variables are maintained at their lower and upper limits during the simulation. A penalty

TABLE 7. Simulation results of case studies 3-5 on IEEE-30 bus test system.

		Case-3			*Case-4*			*Case-5*		
Items	Range	HFO-1a	HFO-1b	HFO-1c	HFO-1a	HFO-1b	HFO-1c	HFO-1a	HFO-1b	HFO-1c
P_1	[80 250]	177.1628	177.1682	177.1668	51.47763	51.47767	51.47765	62.09739	61.55121	55.57605
P_2	[20 80]	48.71658	48.71672	48.71700	80.00000	80.00000	80.00000	80.00000	80.00000	80.00000
P_5	[1550]	21.38130	21.38100	21.38082	50.00000	50.00000	50.00000	49.97398	50.00000	50.00000
P_8	[1035]	21.22127	21.21685	21.21795	35.00000	35.00000	35.00000	34.99939	35.00000	35.00000
P_{11}	[10 30]	11.91552	11.91504	11.91514	30.00000	30.00000	30.00000	29.45178	29.99998	30.00000
P_{13}	[12 40]	12.00000	12.00000	12.00000	40.00000	40.00000	40.00000	30.95278	30.89776	36.78362
V_1	[0.95 1.1]	1.08312	1.08335	1.08334	1.06137	1.06133	1.06143	1.00188	1.00265	0.99960
V_2	[0.95 1.1]	1.02415	1.04434	1.04432	1.01731	1.02727	1.04737	1.00090	1.00198	0.99897
V_5	[0.95 1.1]	1.03297	1.03317	1.03314	1.03787	1.03780	1.03790	1.01888	1.01923	1.01925
V_8	[0.95 1.1]	1.05777	1.04792	1.04792	1.06423	1.04415	1.04425	1.00383	1.01472	1.00546
V_{11}	[0.95 1.1]	1.06102	1.07159	1.07057	1.05618	1.05648	1.05678	1.00883	0.99813	0.99560
V_{13}	[0.95 1.1]	1.04388	1.04147	1.04393	1.05340	1.05395	1.05316	1.02187	1.01577	1.02009
$Q_{c\text{-}10}$	[0 5.0]	3.43827	0.00010	0.00046	0.00092	0.00000	0.00024	5.00000	5.00000	5.00000
$Q_{c\text{-}12}$	[0 5.0]	2.23110	3.16750	1.37698	2.11943	1.83925	2.03052	1.01029	4.99046	4.18103
$Q_{c\text{-}15}$	[0 5.0]	4.35911	4.44627	4.39958	4.58350	4.59044	4.62473	5.00000	5.00000	5.00000
$Q_{c\text{-}17}$	[0 5.0]	5.00000	5.00000	5.00000	5.00000	5.00000	5.00000	0.00000	0.00000	0.00000
$Q_{c\text{-}20}$	[0 5.0]	4.29026	4.24931	4.26773	4.21658	4.19954	4.19751	5.00000	5.00000	5.00000
$Q_{c\text{-}21}$	[0 5.0]	5.00000	5.00000	5.00000	5.00000	5.00000	5.00000	5.00000	5.00000	5.00000
$Q_{c\text{-}23}$	[0 5.0]	3.17476	3.13633	3.14856	3.15581	3.14117	3.13956	5.00000	5.00000	5.00000
$Q_{c\text{-}24}$	[0 5.0]	5.00000	5.00000	5.00000	5.00000	5.00000	5.00000	5.00000	5.00000	5.00000
$Q_{c\text{-}29}$	[0 5.0]	2.02983	2.04403	2.03743	1.91333	1.91813	1.92277	2.57815	2.57714	2.42226
T_{11}	[0.9 1.1]	1.01914	1.02280	1.02932	1.04317	1.04295	1.04358	1.02202	1.01064	1.00729
T_{12}	[0.9 1.1]	0.93408	0.92600	0.91794	0.90000	0.90000	0.90000	0.90000	0.90000	0.90000
T_{15}	[0.9 1.1]	0.96590	0.96415	0.96425	0.99029	0.99067	0.98975	1.00082	0.99969	1.00736
T_{16}	[0.9 1.1]	0.97148	0.97164	0.97161	0.97448	0.97443	0.97457	0.96739	0.96734	0.96538
Q_1	[-20 150]	7.9831	3.2597	1.0132	-3.8283	-7.3575	-10.9280	-6.3633	-17.2876	-15.5576
Q_2	[-20 60]	16.3940	18.4091	19.6420	11.8772	4.9164	10.9000	26.4695	-13.3268	2.9095
Q_5	[-15 62.5]	27.1299	24.8662	25.6265	22.6164	22.4377	18.0134	52.7773	60.2476	51.9837
Q_8	[-15 48.7]	30.1480	28.8870	26.3478	29.9670	24.7775	20.0043	-1.0138	39.4529	37.2738
Q_{11}	[-10 40]	2.6029	1.8603	5.1193	-3.1945	2.7181	16.3814	21.0952	17.7895	31.9792
Q_{13}	[-15 44.7]	-2.3705	9.0874	7.2247	4.7868	14.1702	11.8240	-4.9037	9.5229	-9.6807
f_C($/h)		800.3874	800.3871	**800.3871**	967.6090	967.6091	967.6091	947.5313	948.5859	961.6279
f_{PL}(MW)		8.99752	8.99786	8.99776	**3.07763**	3.07767	3.07765	4.07532	4.04894	3.95967
f_{VD} (p.u)		0.91647	0.91987	0.91819	0.90633	0.90709	0.90694	0.08413	0.08403	**0.08350**

technique is applied to ensure that the generator operates within the safe region. Table8 shows that HFO-1c achieves the best result at $800.6650/h. Additionally, Fig. 11 illustrates HFO-1c's typical behavior of slow convergence. Although HFO-1c has a slower convergence rate, it performs better in finding the optimum points than the HFO-1a variant, which converges the fastest but gets stuck in local points in the process.

According to the results stated in Tables 7 and 8 for this test system, the voltage values of the load busbars for each situation are plotted in Figures 12 and 13. It is imperative to prevent limit violations in the OPF problem. These graphs provide a detailed representation that the load buses voltages are kept in the [0.95-1.05] p.u range in the optimal solution set obtained with HFO-1 variants for each objective function. For the safety of power systems, the voltage amplitudes of all buses must never exceed the permissible limits. A careful examination of Figures 12 and 13, it becomes evident that the bus voltages frequently approach their limits, particularly in cases 3-6 and 8 due to constraints on the load bus voltages. This graph presents a detailed representation of the safety limit values determined load buses in the optimal solution set obtained by HFO-1 variants for each objective function.

Another important issue for the security of the system is that the reactive power values produced by the generators remain within the specified upper and lower limits. In this study, it is shown clearly in Tables 7 and 8 that the generators are kept within the safe operating range. Even in case study 8, which introduced an additional restriction for the operating range of the generators, the penalty technique applied successfully kept all control variables within the limit values and safety restrictions were not violated. If Tables 7 and 8 are examined separately, it is a remarkable result that the control variables as well as the generator reactive power values have

TABLE 8. Simulation results of case studies 6-8 on IEEE-30 bus test system.

		Case-6			*Case-7*			*Case-8*		
Items	Range	HFO-1a	HFO-1b	HFO-1c	HFO-1a	HFO-1b	HFO-1c	HFO-1a	HFO-1b	HFO-1c
P_1	[80 250]	140.0000	140.0000	140.0000	219.8158	219.8158	219.8158	179.3637	179.3644	179.3652
P_2	[20 80]	55.00000	55.00000	55.00000	27.60939	27.60993	27.60881	45.00000	45.00000	45.0000
P_5	[1550]	24.10729	24.15998	24.16420	15.70100	15.70043	15.70149	21.53638	21.53681	21.5365
P_8	[1035]	35.00000	34.99998	35.00000	10.00000	10.00000	10.00000	22.24228	22.24209	22.2415
P_{11}	[10 30]	18.48354	18.43645	18.45884	10.00000	10.00000	10.00000	12.26873	12.26792	12.2679
P_{13}	[12 40]	17.52124	17.51413	17.48710	12.00000	12.00000	12.00000	12.00000	12.00000	12.0000
V_1	[0.95 1.1]	1.07564	1.07609	1.07576	1.09028	1.09046	1.09044	1.08343	1.08342	1.08344
V_2	[0.95 1.1]	1.04093	1.04132	1.04102	1.08576	1.08592	1.09589	1.04401	1.02400	1.04402
V_5	[0.95 1.1]	1.03239	1.03280	1.03252	1.03183	1.03196	1.03194	1.03296	1.03295	1.03298
V_8	[0.95 1.1]	1.04104	1.04132	1.05104	1.03502	1.03513	1.03512	1.04801	1.05800	1.04803
V_{11}	[0.95 1.1]	1.05884	1.06665	1.05863	1.06761	1.07202	1.07054	1.06779	1.06181	1.07419
V_{13}	[0.95 1.1]	1.04581	1.04280	1.04770	1.03866	1.03801	1.03806	1.04150	1.04566	1.04058
$Q_{c\text{-}10}$	[0 5.0]	4.26130	1.55433	3.46850	4.17230	1.40916	2.22350	2.73135	3.75561	0.00486
$Q_{c\text{-}12}$	[0 5.0]	3.55849	4.05505	1.67559	2.35464	2.22830	2.23988	3.22757	0.11160	3.81500
$Q_{c\text{-}15}$	[0 5.0]	4.36178	4.41958	4.44238	4.44838	4.48580	4.51125	4.43117	4.43573	4.44271
$Q_{c\text{-}17}$	[0 5.0]	5.00000	5.00000	5.00000	5.00000	5.00000	4.99999	5.00000	5.00000	5.00000
$Q_{c\text{-}20}$	[0 5.0]	4.22100	4.25436	4.25663	4.23483	4.24763	4.22577	4.25538	4.25678	4.25112
$Q_{c\text{-}21}$	[0 5.0]	5.00000	5.00000	5.00000	5.00000	5.00000	5.00000	5.00000	5.00000	5.00000
$Q_{c\text{-}23}$	[0 5.0]	3.18005	3.13677	3.10640	3.15183	3.13521	3.12994	3.12872	3.13536	3.13253
$Q_{c\text{-}24}$	[0 5.0]	5.00000	5.00000	5.00000	5.00000	5.00000	5.00000	5.00000	5.00000	5.00000
$Q_{c\text{-}29}$	[0 5.0]	2.02087	1.97726	2.01959	2.05489	2.05132	2.04978	2.04373	2.04428	2.04381
T_{11}	[0.9 1.1]	0.99736	1.00924	1.01118	0.99631	1.01148	1.00854	1.00242	1.01605	1.00807
T_{12}	[0.9 1.1]	0.96228	0.94372	0.94114	0.97150	0.94578	0.95123	0.95696	0.93926	0.94489
T_{15}	[0.9 1.1]	0.97466	0.97106	0.97391	0.95614	0.95486	0.95500	0.96426	0.96431	0.96409
T_{16}	[0.9 1.1]	0.97215	0.97217	0.97204	0.97116	0.97121	0.97118	0.97160	0.97156	0.97158
Q_1	[-20 150]	8.0972	3.2858	-0.4767	13.4506	8.7665	18.7290	2.9010	2.9090	2.9088
Q_2	[-20 60]	15.4162	14.9476	11.1205	24.6506	28.2277	15.8661	20.2619	20.2294	20.2601
Q_5	[-15 62.5]	25.5628	26.6148	26.7627	25.6204	16.5439	18.2380	25.6487	25.6495	25.6510
Q_8	[-15 48.7]	28.1894	33.5479	31.0478	20.9132	25.5265	19.4601	26.5645	26.5356	26.5493
Q_{11}	[-10 40]	3.7118	-1.6714	1.9196	-8.5933	8.4497	9.1579	9.7314	9.2340	12.9982
Q_{13}	[-15 44.7]	-6.0546	-10.4239	3.3608	19.3157	6.0177	12.0797	-6.2333	-3.1490	-6.9113
f_C(\$/h)		646.3765	**646.3758**	646.3759	823.9815	**823.9813**	**823.9813**	800.6651	800.6652	**800.6650**
f_{PL}(MW)		6.71206	6.71055	6.71013	11.72621	11.72618	11.72612	9.01118	9.01123	9.01126
f_{VD} (p.u)		0.93466	0.93766	0.93403	0.90110	0.89896	0.89923	0.92439	0.91962	0.92523

different values in the same target function. This situation is especially evident in shunt capacitance values. These differences are due to the different nature of HFO-1 variants. In general, since HFO-1a mixes from random new solutions in the mixing phase, its exploration power is better, whereas HFO-1b, which mixes from existing solutions, has better exploitation power. However, since HFO-1c is an extension of HFO-1a, its exploration power is as good as HFO-1a and, at the same time, the proposed solution update line increases its exploitation power, making it an approach that provides a balance between both exploration and exploitation. The variants have the potential to be superior to one another against different problems. In power problems, situations with multiple local optima (such as fuel cost with valve point effect, power loss) arise due to sinusoidal expressions, making the HFO-1c and HFO-1a approaches, which have high exploration power, more prominent. For problems that create one or a few local optima (such as fuel cost, multi-fuel cost, voltage deviation), the exploit feature is important, so in these problems, HFO-1b and HFO-1c come to the forefront.

In this study, comparison was made with studies in the same category in a transparent manner, strictly adhering to system restrictions, and the results are given in Tables 9 and 10. The works in literature generally blindly compare various optimization algorithms in achieving the OPF problem by using different search ranges (lower and upper limits) for the same variables (solution variables or constraint variables). Furthermore, many studies even do not provide sufficient results or search ranges for the variables such that validations of their feasibilities are not possible. For this reason, among the studies that appear to be superior to the method we suggested in the tables, marks have been placed on studies that cannot be verified or that have constraint violations.

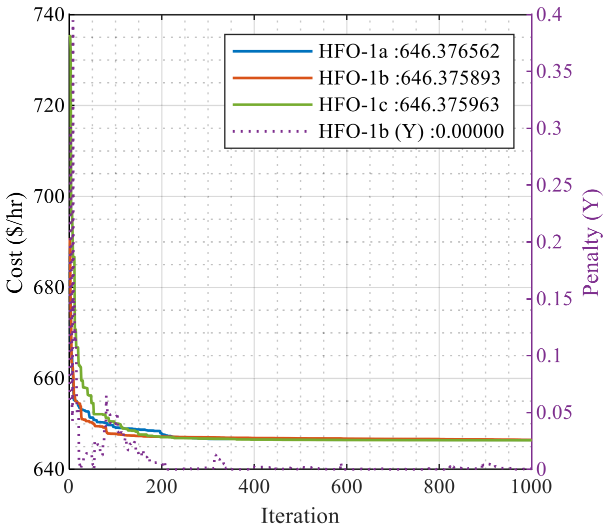

FIGURE 9. Multi-fuel cost convergence of HFO-1a, HFO-1b and HFO-1c for the modified test system.

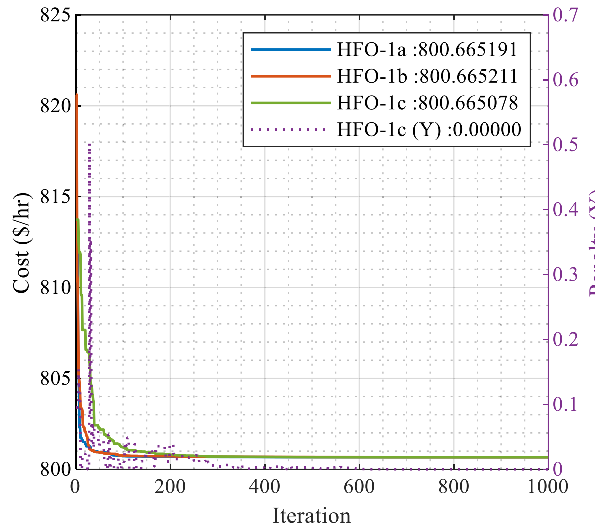

FIGURE 11. Prohibited zone with cost convergence of HFO-1a, HFO-1b and HFO-1c for the modified test system.

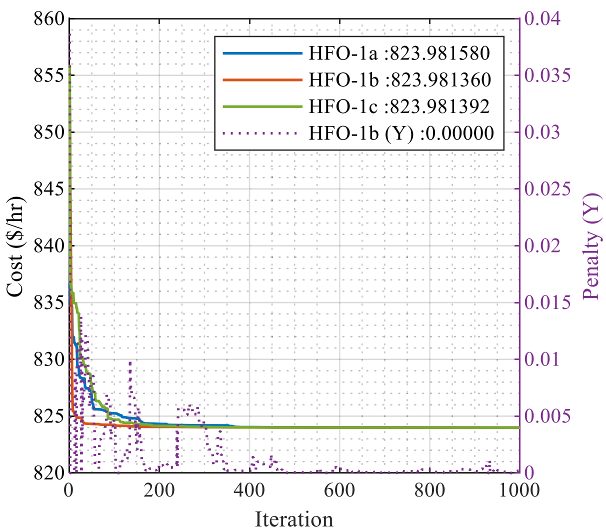

FIGURE 10. Valve effect fuel cost convergence of HFO-1a, HFO-1b and HFO-1c for the modified test system.

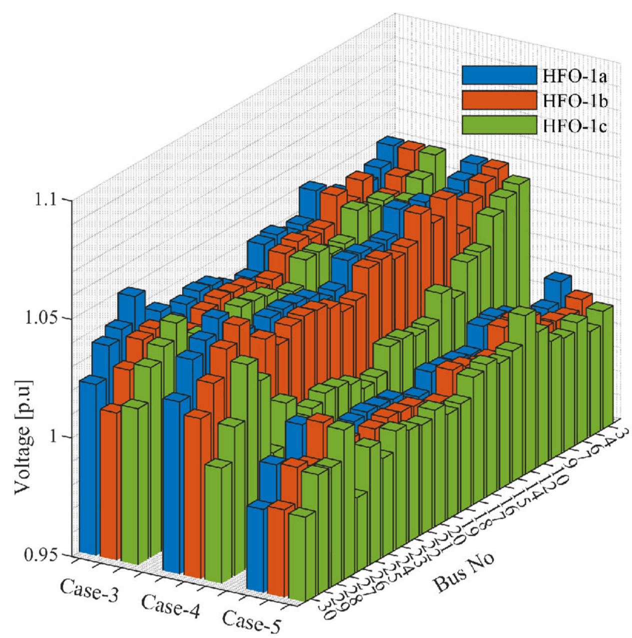

FIGURE 12. Load bus voltage chart for cases 3-5 for the modified test system.

In Table 9, the best-obtained results by the proposed approach are compared with the results reported in the literature regarding cases 3-5. A quick comparison of Table 9 reveals that IMFO, DSA, and IBSA achieve the best fitness values for case 3. Also, ACDE, IBAC, and COA achieve good results for all three cases even though the case 1 results of these algorithms are not the most satisfying. On the other hand, some literature results such as TLBO, ST-IWO, and WEA achieve lower results, but the solution sets of these results are unfortunately out of constraints as given in footnote of Table 9. In this study, HFO-1c achieves the best results for case 1 and case 2 while HFO-1a converges to the best result for case 2, respectively. Also, it can be reported that the IMFO algorithm has a better result for case 3 than the proposed HFO method with a %0.00028 variation, while the HFO-1c algorithm has a better result than IMFO with a %0.41755 variation ratio. Thus, it can be concluded that the HFO-1c algorithm achieves the best result overall for cases 3–5.

For cases 6–8, as compared with other state-of-the-art methods shown in Table10, it is concluded that the HFO-1 variants outperform most of the other reported methods. In Table10, the comparison is presented in detail. For cases 6–8, FAHSPSO-DE and IMFO achieved the best results for case 6. Also, FAHSPSO-DE, ESHADE, and CS-GWO obtain the best results for case 6, while HSC-GWO achieves lower

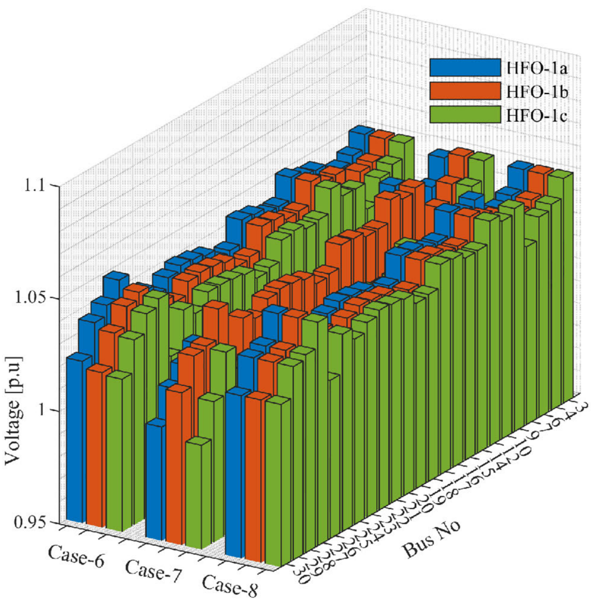

FIGURE 13. Load bus voltage chart for cases 6-8 for the modified test system.

results due to excessing the constraints for some solution parameters. The proposed methodologies, HFO-1a, HFO-1b and HFO-1c achieve better results than most of the literature. All HFO variants converge to the best results compared to other studies presented in the literature for case 8. Therewithal, HFO-1b achieves the best result among HFO variants for case 6 and case 7, while HFO-1c gets the best result for case 8.

In Table 9, it is seen that the proposed HFO variants converge to better results for case 3 when compared most of the studies reported. The HFO-1c variant achieves to best result among HFO variants with 800.387108 $/h fuel cost. If the literature results are investigated, as it is noted below the table some studies namely, AMTPG-JAYA [53], AO-AOA [70], CS-GWO [46], HSC-GWO [69], MGTO [86], ST-IWO [66], LTLBO [44], MSCA [54], TLBO [42], DE-HS [71], WEA [101], ESHADE [64] have converges to better results but voltage deviation values are not reported which raises suspicion that the minimum and maximum limit values of buses are not kept within constraints. Also, for case 4, some literature studies of AO-AOA [70], CS-GWO [46], ST-IWO [66], MSCA [54], DE-HS [71], WEA [101], ESHADE [64] also seems to converge to an infeasible solution due to excessing the limits of voltage constraints. Also, for the results presented in Table 10, it can be concluded that the proposed HFO variants converge to better results for cases 6-8 than most of the studies reported. The HFO-1b variant achieves to best result for cases 6 and 7 while HFO-1c converge to best result for case 8 among HFO variants. In some literature studies, voltage deviation and busbar voltage values are not reported that if those reported results are applied to the current system, the system will fail due to exceeding the constraints. The explanation of such reservations is reported under the table with detail.

TABLE 9. Statistical comparison results for cases 3-5.

Method	Case 3	Case 4	Case 5
HybridSFLA-SA[81]	801.79		
BSA[47]	801.63	3.0844	
WTLBO[43]	800.57	3.109	0.093
GPU-PSO[29]	800.53		
PPSOGSA[102]	800.528	3.10327	0.08986
ARCBBO[32]	800.5159	3.1009	0.092
SKH[49]	800.5141	3.0987	
CGSCE[56]	800.5106	3.1006	
MSA[55]	800.5099	3.1005	
COA[62]	800.5054	3.0952	0.0826
ISSA [61]	800.4752		
IABC[40]	800.4215	3.0917	0.0918
ECHT-DE[23]	800.4131		
ACDE[22]	800.41132	3.084041	0.085636
IeJADE[65]	800.4113	3.0840	0.0856
C2oDE-ECM-FR[103]	800.4112	3.0839	
IBSA[63]	800.3975	3.0828	
DSA[91]	800.3887	3.09450	
IMFO[51]	800.3848	3.0905	
AMTPG-JAYA[53]	800.1946[a]	3.0802	
AO-AOA[70]	800.0239[a1]	3.01791[a1]	0.101248
CS-GWO[46][a]	799.9978[a]	3.0861	
HSC-GWO[69]	799.8755[a2]		
MGTO[86]	799.7888[a3]		
ST-IWO[66]	799.73[a1]	2.981 [a1]	0.1019
LTLBO[44]	*799.4369[a1]*		0.0974
MCSO[60]	*799.3332*		
MSCA[54]	799.31[a1]	2.9334 [a1]	0.1030
TLBO[42]	*799.0715[a2]*		0.0945
DE-HS[71]	799.0514[a]	3.0542[a]	
WEA[101][a2]	798.9969[a2]	2.8604[a2]	0.0875
ESHADE[64][a2]	798.9152[a2]	2.8231[a2]	
HFO-1a	800.387436	**3.077626**	0.084127
HFO-1b	800.387109	3.077670	0.084027
HFO-1c	***800.387108***	3.077649	**0.083498**

[a] voltage deviation not reported Infeasible solution that violates the load bus voltage constraints for (CS-GWO) , (DE-HS) and (MCSO), [a1] voltage deviation 2.047130 p.u Infeasible solution that violates the load bus voltage constraints for (AO-AOA), voltage deviation 1.65739 p.u Infeasible solution that violates the load bus voltage constraints for (ST-IWO) , voltage deviation 1.0829 p.u Infeasible solution that violates the load bus voltage constraints for (LTLBO), voltage deviation 1.5987 p.u Infeasible solution that violates the load bus voltage constraints for (MSCA) [a2]: load bus voltage ranges different [0.95-1.1] for (HSC-GWO) ,(WEA), (TLBO) and (ESHADE) [a3]: not validated because control variables were not provided.

c: THE RENEWABLE INTEGRATED MODIFIED SYSTEM

In this section, similar to other studies presented in the literature, two wind farms and one solar system are integrated into the IEEE 30 bus test system instead of thermal generators 5-11 and 13, respectively [85]. For predicting the wind power

TABLE 10. Statistical comparison results for cases 6-8.

Method	Case 6	Case 7	Case 8
TLBO[42]	647.9202	-	-
LTLBO[44]	647.4315	-	-
MSA[55]	646.8364	-	-
CGSCE[56]	646.5803	-	-
ECHT-DE[23]	646.4314	832.0882	
IeJADE[65]	-	832.0698	-
HSC-GWO[69]	646.4314	806.2255	
C2oDE-ECM-FR[103]	646.402	832.071	
MGTO [86] [a]	646.3025[a]	832.0394	800.1129[a]
IMFO[51][a]	645.8958[a]	832.1023	
FAHSPSO-DE[72][a]	644.0444[a]	820.7488[a]	804.8937
MCSO[60]	-	833.8211	-
IBSA[63]	-	832.1423	-
ACDE[22]	-	832.0722	-
ST-IWO[66]	-	830.222	-
Hybrid SFLA-SA[81]	-	825.6921	805.815
WEA[101]	-	825.2833	801.7703
BSA[47]	-	825.23	801.85
DE-HS[71]	-	824.9963	-
ISSA[61]	-	824.1859	800.8417
CS-GWO[46][a1]	-	823.4304[a2]	-
ESHADE[64][a2]	-	822.5304[a2]	-
HFO-1a	646.376562	823.981580	800.665191
HFO-1b	**646.375893**	**823.981360**	800.665211
HFO-1c	646.375963	823.981392	**800.665078**

[a] control variables not reported therefore not verified (IMFO), (FAHSPSO-DE) and (MGTO) , [a1] Infeasible solution that violates the load bus voltage constraints for (CS-GWO) , [a2]load bus voltage ranges different [0.95-1.1] for (HSC-GWO) ,(WEA), (TLBO) and (ESHADE).

depending on the wind speed, Weibull probability density function (PDF) is used. The Weibull PDF has 2 parameters namely c and k which are scale and shape factor, respectively. Also, in order to present the Weibull PDF of wind farm, the parameters of v_{in}, v_r and v_{out} which are cut-in, rated and cut-out speed should be determined. In this study, the wind generators are planned to be replaced in IEEE 30 bus power system instead of thermal generators in buses 5 and 11. The output of the solar PV unit at bus 13 is dependent upon solar radiation and is represented by a lognormal probability density function (PDF) function. The probability of solar irradiance (G) following lognormal PDF with mean μ and standard deviation σ is:

$$f_G(G) = \frac{1}{G\sigma\sqrt{2\pi}} exp\left\{\frac{-(ln\, x-\mu)^2}{2\sigma^2}\right\} for\ G > 0 \tag{36}$$

Mean of lognormal distribution is defined as:

$$M_{lgn} = exp\left(\mu + \frac{\sigma^2}{2}\right) \tag{37}$$

TABLE 11. Renewable system parameters of wind farms and pv plant considered for IEEE-30 bus test system.

Turbin and PDF parameters	Wind Farms Bus no 5	Wind Farms Bus no 11	PV Plant Bus no 13
v_{in}(m/s)	3	3	
v_r(m/s)	16	16	
v_{out}(m/s)	25	25	
Rated power[MW]	75	60	50
c – Weibull	9	10	
k – Weibull	2	2	
Solar irradiance[W/m^2]			483
μ and σ			6 and 0.6

In wind power integration, if the wind farm produces less power than scheduled amount, a problem may occur due to overestimating power from an uncertain source. For such situations, the system must operate out of schedule in order to provide the customers with uninterrupted supply. For wind farms, the reserve cost is the price of dedicating the reserve generating units to cover the overestimated amount. Another situation of operating wind farms is producing more power than scheduled amount. The excessive power would be wasted in such cases where the operator pays up penalty cost according to agreements [85]. In this study the direct wind power cost along with penalty and reserve cost is utilized. The direct cost function of wind farms along with the reserve and penalty functions are given in equations (38)-(40), respectively.

$$C_{w,j}\left(P_{ws,j}\right) = g_j P_{ws,j} \tag{38}$$

$$C_{Rw,j}\left(P_{ws,j} - P_{wav,j}\right) = K_{Rw,j}\left(P_{ws,j} - P_{wav,j}\right) = K_{Rw,j}\int_0^{P_{wsj}}\left(P_{ws,j} - p_{w,j}\right) f_w\left(p_{w,j}\right) dp_{w,j} \tag{39}$$

$$C_{P_{w,j}}\left(P_{wav,j} - P_{ws,j}\right) = K_{Pw,j}\left(P_{wav,j} - P_{ws,j}\right) = K_{Pw,j}\int_{P_{ws,j}}^{P_{w,j}}\left(p_{w,j} - P_{ws,j}\right) f_w\left(p_{w,j}\right) dp_{wj} \tag{40}$$

where, g_j, $K_{Rw,j}$ and $K_{Pw,j}$ are the direct cost coefficient, the reserve cost coefficient and the penalty cost coefficient for the j-th wind power plant, respectively. $P_{ws,j}$, $P_{wav,j}$ and $f_w\left(p_{w,j}\right)$ are the scheduled power, the actual available power and the wind power probability density function associated with j-th from the same plant, respectively. The total cost of wind power (f_{cw}) generated from wind farms is described as follows;

$$f_{cw} = \sum_{j=1}^{N_{wG}}\left[C_{w,j}\left(P_{wsjj}\right) + C_{Rw,j}\left(P_{ws,j} - P_{wwv,j}\right) + C_{Pwj}\left(P_{wwv,j} - P_{ws,j}\right)\right] \tag{41}$$

Like wind power plant, solar PV plant also have intermittent and uncertain output. In principle, approach to over and under

TABLE 12. Results of case 9 on the IEEE-30 bus renewable integrated modified test system.

		Existing methods						*Case-9*		
Items	Range	MFO[106]	JS[107]	DMOA[108]	BMO[109]	IEO[110]	SHADE-SF[85]	HFO-1a	HFO-1b	HFO-1c
P_{G1}	[50 140]	134.90	134.905	134.914	134.9078	134.9079	134.908	134.9079	134.9079	134.9079
P_{G2}	[20 80]	28.471	29.0226	27.6003	26.6024	27.8087	28.564	28.52549	28.73079	28.85885
P_{Gwind1}	[0 75]	44.644	43.9696	43.1838	43.8165	44.0873	43.774	43.78191	43.8050	43.69028
P_{G8}	[10 35]	10.000	10.0006	10.0180	10.0001	10.0000	10	10.00014	10.00000	10.00002
P_{Gwind2}	[0 60]	36.588	37.0193	35.8046	36.0467	36.2702	36.949	37.21641	36.99769	36.98909
P_{Gsolar}	[0 50]	34.460	34.2532	37.6001	37.8118	36.3030	34.976	34.43360	34.42937	34.42959
V_1	[0.95 1.1]	1.0798	1.07725	1.0741	1.0814	1.0766	1.072	1.079900	1.079032	1.079396
V_2	[0.95 1.1]	1.0647	1.05698	1.0576	0.95	1.0592	1.057	1.044519	1.033500	1.023908
V_5	[0.95 1.1]	1.0428	1.03507	1.0344	1.0453	1.0338	1.035	1.052199	1.060782	1.071125
V_8	[0.95 1.1]	1.1	1.03705	1.0394	1.0492	1.0299	1.04	1.054917	1.054222	1.054610
V_{11}	[0.95 1.1]	1.1	1.0983	1.0951	1.1000	1.0887	1.1	1.059356	1.060292	1.058946
V_{13}	[0.95 1.1]	1.0583	1.04571	1.0531	1.0680	1.0494	1.055	1.042861	1.048435	1.047794
Q_{G1}	[-20 150]	-1.4418	-0.6835	1.67529	18.0500	-	-	-0.09491	-0.28628	-0.16883
Q_{G2}	[-20 60]	12.139	11.0011	10.9737	-20.000	-	-	12.93923	12.10517	12.43564
Q_{Gwind1}	[-30 35]	22.405	22.6673	2.18057	30.3440	-	-	22.70875	22.21903	22.18495
Q_{G8}	[-15 48.7]	40.00	40.000	33.3277	40.000	-	-	26.16270	26.69810	26.62275
Q_{Gwind2}	[-25 30]	28.294	30.00	28.1558	27.8687	-	-	8.566096	6.883986	7.405196
Q_{Gsolar}	[-20 25]	14.436	14.0246	15.73256	19.9978	-	-	4.560327	-0.41858	-0.89662
f_C($/h)		781.69	782.6767	780.989	781.6519	782.0343	782.503	781.1702	781.1217	**781.0787**
f_{PL}(MW)		-	-	5.7209	-	5.9771	5.770	5.472571	5.575898	5.580408
f_{VD} (p.u)		-	-	0.46464	-	-	0.463	1.040979	0.972986	0.971495

estimation of solar power shall be same as the wind power. However, as solar radiation follows lognormal PDF [104], different from wind distribution which is well known for trailing Weibull PDF, for convenience in calculation the reserve and penalty cost models are built based on the concept presented in [105].

Reserve cost for the$k$-th solar PV plant is:

$$\begin{aligned} C_{Rs,k}\left(P_{ss,k}-P_{sav,k}\right) &= K_{Rs,k}\left(P_{ss,k}-P_{sav,k}\right) \\ &= K_{Rs,k}{}^{*}f_s\left(P_{sav,k}<P_{ss,k}\right) \\ &\quad \times{}^{*}\left[P_{ss,k}-E\left(P_{sav,k}<P_{ss,k}\right)\right] \end{aligned} \tag{42}$$

where, $K_{Rs,k}$ is the reserve cost coefficient pertaining to k-th solar PV plant, $P_{sav,k}$ is the actual available power from the same plant. $f_s\left(P_{sav,k}<P_{ss,k}\right)$ is the probability of solar power shortage occurrence than the scheduled power $\left(P_{ss,k}\right)$, $E\left(P_{sav,k}<P_{ss,k}\right)$ is the expectation of solar PV power below $P_{ss,k}$.

Penalty cost for the underestimation of k-th solar PV plant is:

$$\begin{aligned} C_{Ps,k}\left(P_{sav,k}-P_{ss,k}\right) &= K_{Ps,k}\left(P_{sav,k}-P_{ss,k}\right) \\ &= K_{Ps,k}{}^{*}f_s\left(P_{sav,k}>P_{ss,k}\right) \\ &\quad \times{}^{*}\left[E\left(P_{sav,k}>P_{ss,k}\right)-P_{ss,k}\right] \end{aligned} \tag{43}$$

where, $K_{Ps,k}$ is the penalty cost coefficient pertaining to k-th solar PV plant, $f_s\left(P_{sav,k}>P_{ss,k}\right)$ is the probability of solar power surplus than the scheduled power $\left(P_{ss,k}\right)$, $E\left(P_{sav,k}>P_{ss,k}\right)$ is the expectation of solar PV power above $P_{ss,k}$.

The objective of OPF is formulated by incorporating all the cost functions as discussed above.

$$\begin{aligned} f_{c(TG+WG+SG)} = & C_T\left(P_{TG}\right)+\sum\nolimits_{j=1}^{N_{wG}}\left[C_{w,j}\left(P_{ws,j}\right)\right. \\ & +C_{Rw,j}\left(P_{ws,j}-P_{wavv,},\right. \\ & \left.+C_{Pw,j}\left(P_{wav,j}-P_{wsj}\right)\right] \\ & +\sum\nolimits_{k=1}^{N_{sG}}\left[C_{s,k}\left(P_{ss,k}\right)\right. \\ & +C_{Rs,k}\left(P_{ss,k}-P_{sav,k}\right) \\ & \left.+C_{Dct}\left(P_{cav,}-P_{cct}\right)\right] \end{aligned} \tag{44}$$

where, N_{WG} and N_{SG} are the numbers of wind generators and solar PVs in the network respectively. All other cost components are calculated using Eqs. (38)- (43).

A Monte Carlo simulation with 10,000 iterations can be used to determine the distribution of wind speed and solar radiation frequency at buses 5, 11, and 13, utilizing the Weibull and Lognormal parameters provided in Table 11. During the simulation, in addition to the turbine and PDF parameters given in Table 11, the direct cost coefficients of wind power are $g_1 = 1.6$ and $g_2 = 1.75$. The penalty cost coefficient for not fully utilizing wind power is assumed to be $K_{Pw,1} = K_{Pw,2} = 1.5$, while the reserve cost coefficient for overestimation is $K_{Rw,1} = K_{Rw,2} = 3$. Accordingly, for the purposes of this study, the direct, penalty, and reserve cost coefficients for solar PV are assumed to be $h = 1.6$, $K_{Ps} = 1.5$, and $K_{Rs} = 3$, respectively.

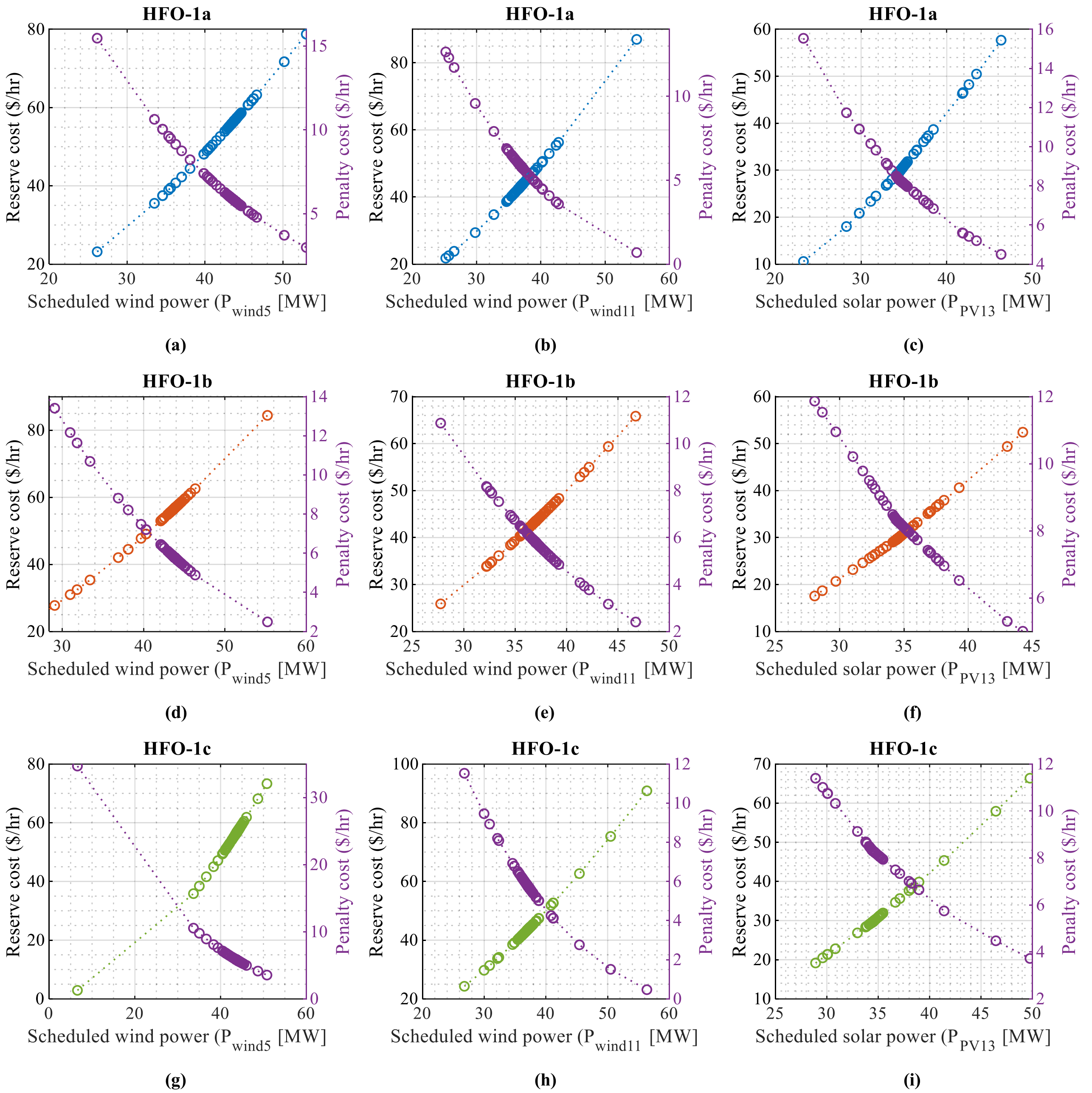

FIGURE 14. Graphs of reserve and penalty costs of renewable resources using HFO-1a, b, c algorithms for case 9 in the modified test system.

Detailed optimal results of control and status variables obtained by HFO-1 variants are given in Table 12. HFO-1c achieved the lowest production cost at $781.0787/h and is highlighted in bold. This result is the lowest value compared to other methods, except DMOA. All variants of the HFO-1 algorithm have shown that they can be recommended as a solution to this problem by showing superior performance without violating all system constraints, despite the negative impact of the uncertainty of renewable resources. In addition, the proposed HFO-1 variants have also managed to keep renewable generators away from the maximum reactive power limit values. While the wind turbine at bus number 11 relies on the upper limit in the JS method and produces reactive power very close to the upper limit in other methods, the proposed method reaches 8.566 MVar with the highest HFO-1a variant. It produces reactive power. While the solar generator placed on busbar 13 worked in the region close to the upper limit value in other algorithms, variants of the proposed algorithm produced reactive power at lower values. This result is especially important in keeping renewable generators away from a strenuous working environment.

TABLE 13. Simulation results of case study 10 on IEEE-118 bus test system.

	Case-10										
Items	HFO-1a	HFO-1b	HFO-1c	Items	HFO-1a	HFO-1b	HFO-1c	Items	HFO-1a	HFO-1b	HFO-1c
P_{G1}	24.32766	25.05435	24.57541	P_{G103}	38.24908	38.25431	38.26337	V_{G80}	1.05982	1.05896	1.06000
P_{G4}	0.00000	0.00000	0.00000	P_{G104}	0.00022	0.00000	0.00000	V_{G85}	1.05108	1.05101	1.05141
P_{G6}	0.00001	0.00000	0.00001	P_{G105}	5.44887	5.58367	5.50977	V_{G87}	1.05421	1.05250	1.05632
P_{G8}	0.00000	0.00000	0.00000	P_{G107}	29.27697	29.23803	29.27508	V_{G89}	1.06000	1.06000	1.06000
P_{G10}	401.6865	401.6146	401.5810	P_{G110}	7.18191	7.11000	7.23681	V_{G90}	1.04112	1.04130	1.04147
P_{G12}	85.65998	85.61816	85.65866	P_{G111}	35.24568	35.24061	35.24389	V_{G91}	1.04429	1.04469	1.04501
P_{G15}	19.79957	19.72903	19.79987	P_{G112}	36.63040	36.70794	36.64021	V_{G92}	1.04922	1.04921	1.04954
P_{G18}	12.31951	12.13578	12.27911	P_{G113}	0.00003	0.00000	0.00000	V_{G99}	1.05196	1.05162	1.05257
P_{G19}	20.86661	20.85267	20.80416	P_{G116}	0.00000	0.00000	0.00000	V_{G100}	1.05566	1.05551	1.05642
P_{G24}	0.00001	0.00000	0.00000	V_{G1}	1.03254	1.03256	1.03298	V_{G103}	1.04843	1.04829	1.04935
P_{G25}	194.3462	194.3571	194.3595	V_{G4}	1.05849	1.05891	1.05875	V_{G104}	1.03958	1.03945	1.04057
P_{G26}	280.6217	280.5908	280.5952	V_{G6}	1.05081	1.05092	1.05136	V_{G105}	1.03724	1.03711	1.03827
P_{G27}	10.83565	10.81784	10.82840	V_{G8}	1.04718	1.04781	1.04592	V_{G107}	1.03108	1.03097	1.03215
P_{G31}	7.24710	7.24647	7.24663	V_{G10}	1.05950	1.06000	1.05839	V_{G110}	1.03832	1.03814	1.03942
P_{G32}	15.39175	15.37209	15.42412	V_{G12}	1.04819	1.04801	1.04879	V_{G111}	1.04599	1.04585	1.04713
P_{G34}	3.10272	3.01135	3.09690	V_{G15}	1.04809	1.04808	1.04798	V_{G112}	1.03093	1.03081	1.03210
P_{G36}	9.00367	8.99394	9.06078	V_{G18}	1.05014	1.04984	1.04987	V_{G113}	1.05577	1.05570	1.05563
P_{G40}	48.46866	48.40800	48.49019	V_{G19}	1.04751	1.04737	1.04734	V_{G116}	1.05988	1.05997	1.05960
P_{G42}	40.92712	40.92245	40.97725	V_{G24}	1.05005	1.04997	1.05031	Q_{c-5}	29.99979	29.96964	29.62576
P_{G46}	19.05671	19.05503	19.05962	V_{G25}	1.06000	1.06000	1.06000	Q_{c-34}	2.25391	1.02100	2.61201
P_{G49}	193.7187	193.6640	193.7559	V_{G26}	1.06000	1.06000	1.06000	Q_{c-37}	0.00006	0.00000	0.00000
P_{G54}	49.51155	49.51506	49.51857	V_{G27}	1.04522	1.04515	1.04528	Q_{c-44}	4.29062	4.25050	4.27001
P_{G55}	31.58482	31.55740	31.59530	V_{G31}	1.04082	1.04063	1.04079	Q_{c-45}	20.78510	20.82582	20.84006
P_{G56}	32.08258	32.08863	32.00455	V_{G32}	1.04419	1.04411	1.04424	Q_{c-46}	28.42895	4.30557	23.99922
P_{G59}	149.6313	149.6047	149.6286	V_{G34}	1.05530	1.05521	1.05523	Q_{c-48}	8.53493	8.56260	8.53928
P_{G61}	148.4916	148.5068	148.5124	V_{G36}	1.05367	1.05361	1.05360	Q_{c-74}	29.24289	30.00000	29.96397
P_{G62}	0.00001	0.00000	0.00000	V_{G40}	1.04285	1.04308	1.04325	Q_{c-79}	30.00000	30.00000	30.00000
P_{G65}	353.1999	353.1331	353.1993	V_{G42}	1.04305	1.04288	1.04358	Q_{c-82}	29.99998	29.99874	30.00000
P_{G66}	349.8469	349.7990	349.8500	V_{G46}	1.04433	1.04325	1.04499	Q_{c-83}	11.61554	13.36956	10.99822
P_{G69}	454.8938	454.9118	454.9240	V_{G49}	1.05719	1.05601	1.05795	Q_{c-105}	23.30494	7.64874	10.09674
P_{G70}	0.00002	0.00000	0.00000	V_{G54}	1.04050	1.03937	1.04111	Q_{c-107}	2.33767	25.95351	7.30397
P_{G72}	0.00001	0.00000	0.00000	V_{G55}	1.04055	1.03941	1.04115	Q_{c-110}	18.27795	11.43287	25.64146
P_{G73}	0.00000	0.00000	0.00000	V_{G56}	1.04024	1.03911	1.04085	T_{8}	0.98962	0.99152	0.98961
P_{G74}	17.41448	17.47268	17.45269	V_{G59}	1.05774	1.05698	1.05823	T_{26}	1.05980	1.05976	1.05989
P_{G76}	23.25548	23.00150	22.73241	V_{G61}	1.06000	1.06000	1.06000	T_{30}	0.98573	0.98526	0.98435
P_{G77}	0.00001	0.00000	0.00000	V_{G62}	1.05590	1.05533	1.05590	T_{38}	0.98129	0.98069	0.98027
P_{G80}	431.7840	431.7234	431.8193	V_{G65}	1.06000	1.06000	1.06000	T_{63}	0.98507	0.98579	0.98404
P_{G85}	0.00000	0.00000	0.00000	V_{G66}	1.06000	1.06000	1.06000	T_{64}	0.99695	0.99931	0.99766
P_{G87}	3.63053	3.62743	3.63139	V_{G69}	1.06000	1.06000	1.06000	T_{65}	0.98493	0.98389	0.98548
P_{G89}	502.4463	502.5655	502.4654	V_{G70}	1.03827	1.03743	1.03851	T_{68}	0.95222	0.95144	0.95195
P_{G90}	0.00000	0.00000	0.00000	V_{G72}	1.04114	1.04088	1.04160	T_{81}	0.98782	0.98882	0.98756
P_{G91}	0.00000	0.00000	0.00000	V_{G73}	1.03680	1.03691	1.03792	f_C($/h)	129612.0	129612.5	**129611.7**
P_{G92}	0.00000	0.00000	0.00000	V_{G74}	1.02961	1.02819	1.03004	f_{VC}($/h)	129896.4	129897.1	129898.4
P_{G99}	0.00004	0.00000	0.00000	V_{G76}	1.01384	1.01275	1.01422	f_{VD}(p.u)	2.74527	2.72656	2.76389
P_{G100}	231.3264	231.4265	231.4359	V_{G77}	1.04645	1.04548	1.04709	f_{PL}(MW)	76.51335	76.51229	76.53230

The changes in reserve and penalty costs between zero and nominal power values of each renewable resource are plotted in Figure 14. As expected, the penalty cost decreases while the reserve cost increases. It is seen that the penalty cost of solar power is higher than wind. This can be explained by the fact that the continuity of the wind throughout the year is greater than that of the sun. Among the HFO-1 variants, it is seen that the HFO-1c variant tends to quickly reduce the impact of the penalty cost and thus achieves the lowest cost.

TABLE 14. Simulation results of case study 11 on IEEE-118 bus test system.

	Case-11										
Items	HFO-1a	HFO-1b	HFO-1c	Items	HFO-1a	HFO-1b	HFO-1c	Items	HFO-1a	HFO-1b	HFO-1c
P_{G1}	80.05611	81.27183	80.00273	P_{G103}	22.77146	23.04593	22.85153	V_{G80}	1.01535	1.01519	1.01753
P_{G4}	55.87685	55.58001	56.22252	P_{G104}	37.80757	38.08682	37.94777	V_{G85}	1.01726	1.01673	1.01915
P_{G6}	64.50479	64.35275	64.48562	P_{G105}	64.53180	64.52780	64.69375	V_{G87}	1.02176	1.02125	1.02351
P_{G8}	68.66060	69.14629	68.20814	P_{G107}	57.75206	57.69865	57.66154	V_{G89}	1.01732	1.01630	1.01887
P_{G10}	0.03569	0.04019	0.08178	P_{G110}	44.29136	44.38756	44.12241	V_{G90}	1.01106	1.01029	1.01272
P_{G12}	181.2544	180.9247	180.4028	P_{G111}	0.00005	0.00085	0.02399	V_{G91}	1.01673	1.01623	1.01876
P_{G15}	99.99998	99.99990	99.99949	P_{G112}	67.94846	67.97741	68.12996	V_{G92}	1.01417	1.01342	1.01595
P_{G18}	64.37793	64.56616	64.32752	P_{G113}	11.82663	11.86809	11.96509	V_{G99}	1.01586	1.01552	1.01785
P_{G19}	81.02323	81.07831	81.16897	P_{G116}	99.99972	99.99992	99.99933	V_{G100}	1.01610	1.01568	1.01803
P_{G24}	22.40727	22.32608	22.50549	V_{G1}	0.98380	1.00119	0.99012	V_{G103}	1.01588	1.01570	1.01802
P_{G25}	0.00113	0.00128	0.00828	V_{G4}	0.99521	1.01222	1.00135	V_{G104}	1.01585	1.01574	1.01812
P_{G26}	15.05856	14.88331	14.99381	V_{G6}	0.99508	1.01204	1.00123	V_{G105}	1.01587	1.01577	1.01820
P_{G27}	99.99405	100.0000	99.99757	V_{G8}	0.99374	0.98984	0.99644	V_{G107}	1.01589	1.01576	1.01820
P_{G31}	69.76494	69.80803	69.74164	V_{G10}	0.99305	0.98917	0.99567	V_{G110}	1.01526	1.01551	1.01792
P_{G32}	79.44610	79.15599	79.36888	V_{G12}	0.99495	1.01169	1.00114	V_{G111}	1.01479	1.01540	1.01793
P_{G34}	99.99844	99.99954	99.99998	V_{G15}	0.99630	1.01081	1.00569	V_{G112}	1.01524	1.01548	1.01806
P_{G36}	68.93163	69.75026	70.44532	V_{G18}	0.99718	1.01140	1.00651	V_{G113}	0.99844	1.01213	1.00732
P_{G40}	99.99997	100.0000	99.99998	V_{G19}	0.99743	1.01178	1.00721	V_{G116}	0.99454	0.99129	1.00044
P_{G42}	99.99994	99.99999	99.99998	V_{G24}	1.00274	1.01164	1.01030	$Q_{c\text{-}5}$	16.27997	29.99404	17.68599
P_{G46}	82.36634	82.27933	82.33181	V_{G25}	1.00101	1.01138	1.00911	$Q_{c\text{-}34}$	0.00002	0.00005	0.00078
P_{G49}	190.2765	190.4822	190.5173	V_{G26}	0.99445	0.99014	0.99807	$Q_{c\text{-}37}$	0.00000	0.00005	0.00098
P_{G54}	147.9998	147.9998	147.9997	V_{G27}	1.00031	1.01181	1.00880	$Q_{c\text{-}44}$	4.48491	4.59886	4.50976
P_{G55}	79.41112	79.10196	79.40178	V_{G31}	0.99963	1.01183	1.00826	$Q_{c\text{-}45}$	20.82131	20.17246	20.28542
P_{G56}	99.99997	99.99997	100.0000	V_{G32}	1.00023	1.01164	1.00871	$Q_{c\text{-}46}$	9.82642	22.63646	6.71549
P_{G59}	254.9999	255.0000	254.9999	V_{G34}	0.99922	1.01319	1.01327	$Q_{c\text{-}48}$	8.02782	7.98224	7.95897
P_{G61}	80.26735	79.74367	79.84576	V_{G36}	0.99689	1.01110	1.01173	$Q_{c\text{-}74}$	28.66283	24.64927	25.95489
P_{G62}	99.99773	99.99996	99.99795	V_{G40}	0.99780	1.00970	1.01115	$Q_{c\text{-}79}$	29.99926	29.99996	29.99862
P_{G65}	43.33675	44.35319	44.75392	V_{G42}	1.00164	1.01050	1.01340	$Q_{c\text{-}82}$	29.99998	29.99997	29.99605
P_{G66}	52.43492	51.82491	51.85485	V_{G46}	1.01254	1.01601	1.02068	$Q_{c\text{-}83}$	10.91604	10.80980	10.82635
P_{G69}	59.07643	58.44513	58.62762	V_{G49}	1.01193	1.01495	1.02010	$Q_{c\text{-}105}$	12.02803	25.55133	6.05299
P_{G70}	77.99957	77.42021	77.87662	V_{G54}	1.01276	1.01415	1.02064	$Q_{c\text{-}107}$	26.02243	6.11702	0.24165
P_{G72}	11.98713	12.04126	12.04937	V_{G55}	1.01306	1.01437	1.02094	$Q_{c\text{-}110}$	6.35837	4.36812	12.41068
P_{G73}	6.06089	5.98722	6.12133	V_{G56}	1.01253	1.01380	1.02040	T_{8}	1.00136	0.98377	0.99777
P_{G74}	99.99980	99.99975	99.99927	V_{G59}	1.01192	1.01331	1.01977	T_{26}	1.05567	1.03967	1.04761
P_{G76}	99.99997	99.99963	99.99970	V_{G61}	1.01304	1.01455	1.02047	T_{30}	0.99018	0.97225	0.98528
P_{G77}	99.99998	100.0000	99.99989	V_{G62}	1.01278	1.01435	1.02032	T_{38}	0.98720	0.96796	0.97812
P_{G80}	319.4284	319.4898	318.6359	V_{G65}	0.99508	0.99163	1.00092	T_{63}	0.97834	0.97390	0.97670
P_{G85}	98.11862	98.12603	97.91469	V_{G66}	1.01233	1.01484	1.02023	T_{64}	0.97497	0.96999	0.97339
P_{G87}	11.72889	11.68813	11.73938	V_{G69}	1.01220	1.01205	1.01579	T_{65}	0.96158	0.96023	0.95670
P_{G89}	78.82040	78.50600	78.74751	V_{G70}	1.01097	1.00994	1.01464	T_{68}	0.95586	0.95363	0.95831
P_{G90}	99.99998	100.0000	99.99997	V_{G72}	1.00662	1.01078	1.01221	T_{81}	0.96715	0.96360	0.97016
P_{G91}	37.15532	37.33985	37.23385	V_{G73}	1.01006	1.00988	1.01416	f_C($/h)	166404.3	166415.2	166381.1
P_{G92}	100.0000	99.99998	99.99991	V_{G74}	1.01150	1.00897	1.01475	f_{VC}($/h)	167272.9	167273.2	167241.5
P_{G99}	41.97798	41.90433	41.90558	V_{G76}	0.99877	0.99779	1.00160	f_{VD}(p.u)	0.49936	0.43375	0.49830
P_{G100}	120.1836	119.6245	119.9288	V_{G77}	1.00930	1.00911	1.01148	f_{PL}(MW)	9.94847	**9.83470**	9.83843

2) IEEE 118-BUS SYSTEM

The IEEE-118 bus system has a base apparent power of 100 MVA. The total system demand for active power is 4242 MW, and for reactive power is 1439 MVAR. The coefficients for fuel cost can be found in [48]. This section optimizes fuel cost and active power loss in a large-scale 118 bus test system in cases 10 and 11. Table 13 presents the results of the control variables of HFO-1 variants for case 11. The results indicate that HFO-1c has the lowest cost at 129611.784386 $/h for finding the least cost compared to the other variants. Furthermore, in Fig. 15, HFO-1c demonstrates faster convergence performance compared to the other

TABLE 15. Statistical comparison results for case studies 10 and 11.

Method	Case 10	Case 11
ECHT-DE[23]	135055.7	17.6946
C2oDE-ECM-FR[103]	134943.8	16.79906
IBSA[63]	134941.0367	16.2869
ESHADE[64]	134794.92	15.5318
IMFO[51]	1318200	
NISSO[73]	129879.45361	
MCSO[60]	129873.6	
QRJFS[67]	129760.7	
ESNST[57]	129747.7273	
TLBO[42]	129682.844	
MSA[55]	129640.7191	
GPU-PSO[29]	129627.03	
BA-AMO[75]	129550.8	12.029
CS-GWO[46][a1]	129544.01 [a1]	9.7809 [a1]
AO-AOA[70][a1]	129311.701 [a1]	16.7265
HSC-GWO[69][a2]	128947.961 [a2]	
ST-IWO[66][a2]	128431.035[a2]	
HFO-1a	129612.083023	9.94847
HFO-1b	129612.514527	**9.83470**
HFO-1c	**129611.784386**	9.83843

[a1]Infeasible solution that violates the load bus voltage constraints, [a2]control variables are not reported.

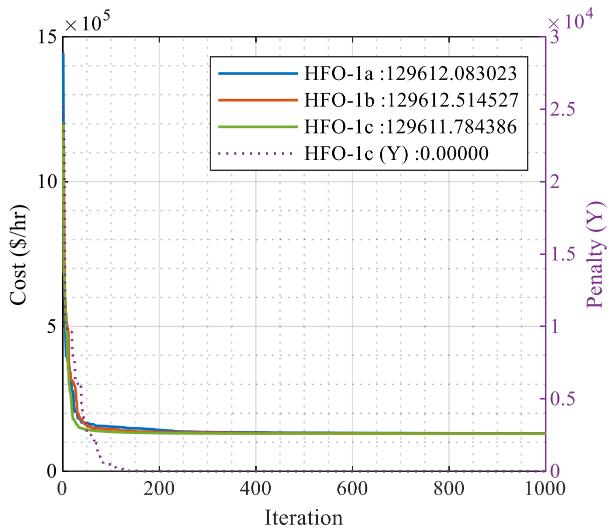

FIGURE 15. Basic fuel cost convergence of HFO-1a, HFO-1b and HFO-1c for 118 bus test system.

variants. Case 11 pertains to the optimization of active power loss in the 118-bus test system. Table 14 presents the results of the HFO-1 variants for case 11. Among the variants, HFO-1b has the lowest active power loss of 9.834698 MW and superior convergence performance, as shown in Fig. 16.

The results of the proposed study for cases 10 and 11 are compared with other proposed methods in the literature and given in Table 15. If results are investigated, it is seen that

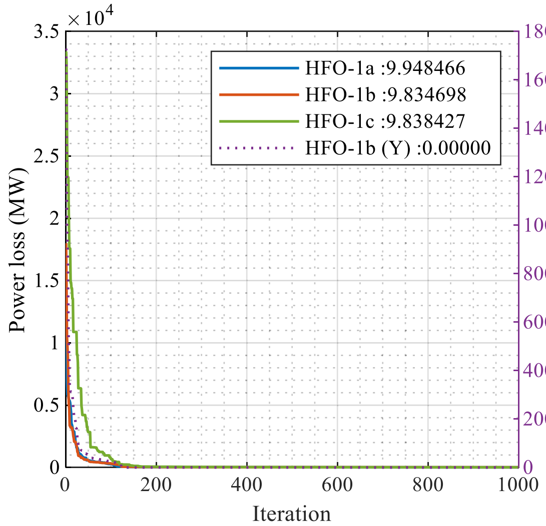

FIGURE 16. Active power loss convergence of HFO-1a, HFO-1b and HFO-1c for 118 bus test system.

case 10 is studied more than case 11. For case 10, ST-IWO has the best result with 128431.035, which is followed by HSC-GWO and AO-AOA. However, as shown in Table 15, the results of HSC-GWO and AO-AOA are not considered the best solutions due to situations of not reporting the control variables and excessing the bus voltage constraint, respectively. At the same time, CS-GWO reported the best solution for case 11, but this method violates the voltage bus constraint similar to AO-AOA. The proposed variants of HFO converge to the best result compared to other state-of-the-art methodologies in literature except ST-IWO for case 10. Also, the HFO variants converge to the best result in the literature for case 11. If the variants are compared, HFO-1c and HFO-1b obtain the optimal solution sets for case 10 and case 11, respectively, while the results of HFO-1a are also very close to other variants.

V. CONCLUSION

In this study, the HFO-1 algorithm is initially tailored to tackle the OPF problem, followed by the derivation of three new variants HFO-1a, HFO-1b, and HFO-1c. These variants are then benchmarked against state-of-the-art methods for the OPF problem and the CEC 2021 Benchmark Test Suite. The proposed HFO-1 variants not only effectively solve the challenging OPF problem by overcoming all technical and safety constraints of the power system, but also provide exceptional solutions for systems compounded by uncertainties of renewable resources. In general, HFO-1a mixes from random new solutions in the mixing phase, thus, its exploration power is better, whereas HFO-1b, which mixes from existing solutions, has better exploitation power. However, HFO-1c, as an extension to HFO-1a, provides a balance between its exploration and exploitation power using the proposed local search (solution update equation). The variants have the potential to be superior to one another against different problems, and it has been demonstrated that the differences and benefits in the exploration, search and exploitation capabilities of the HFO-1 variants can be used to achieve better convergence of the solution sets of different objective functions to a more optimal solution point. In order to ensure a fair and transparent comparison with the literature, studies with the same constraint ranges were meticulously filtered out from the test systems having the same number of control variables. The developed HFO-1 variants, especially HFO-1c, yield results that surpass the performance of most studies. The penalty technique was employed to adhere rigorously to the constraint values, and the results are elaborately presented. As an equitable benchmarking tool, the voltage deviation is reduced to 0.08350 p.u., an achievement considered the best in the literature with no room for constraint violation. The main contribution of this work is the demonstration that, thanks to the diversity of HFO-1 variants, superior solutions can be obtained for the challenging OPF problem, which has inherently different solutions.

The proposed HFO-1 algorithm has shown promising results. It will play a significant role in the real-time stability and security analysis of power systems in the near future. Furthermore, it will provide researchers with fair and transparent benchmarking results under the same conditions, without compromising the system constraints that we are focused on.

REFERENCES

[1] J. Carpentier, "Contribution a l'etude du dispaching economique," *Bull. Soc. Francaise Electricians*, vol. 8, pp. 431–447, Aug. 1962.

[2] H. Dommel and W. Tinney, "Optimal power flow solutions," *IEEE Trans. Power App. Syst.*, vol. PAS-87, no. 10, pp. 1866–1876, Oct. 1968, doi: 10.1109/TPAS.1968.292150.

[3] K. Y. Lee, Y. M. Park, and J. L. Ortiz, "A united approach to optimal real and reactive power dispatch," *IEEE Power Eng. Rev.*, vol. PER-5, no. 5, pp. 42–43, May 1985, doi: 10.1109/MPER.1985.5526580.

[4] R. Mota-Palomino and V. H. Quintana, "Sparse reactive power scheduling by a penalty function—Linear programming technique," *IEEE Trans. Power Syst.*, vol. PS-1, no. 3, pp. 31–39, Aug. 1986, doi: 10.1109/TPWRS.1986.4334951.

[5] A. A. A. El-Ela and M. A. Abido, "Optimal operation strategy for reactive power control," *Model. Simul. Control A, General Phys. Matter Waves Elect. Electron. Eng.*, vol. 41, no. 3, p. 19, 1992.

[6] R. Burchett, H. Happ, and D. Vierath, "Quadratically convergent optimal power flow," *IEEE Trans. Power App. Syst.*, vol. PAS-103, no. 11, pp. 3267–3275, Nov. 1984, doi: 10.1109/TPAS.1984.318568.

[7] A. J. Santos, "Optimal-power-flow solution by Newton's method applied to an augmented Lagrangian function," *IEE Proc. Gener., Transmiss. Distrib.*, vol. 142, no. 1, pp. 33–36, 1995.

[8] D. Sun, B. Ashley, B. Brewer, A. Hughes, and W. Tinney, "Optimal power flow by Newton approach," *IEEE Trans. Power App. Syst.*, vol. PAS-103, no. 10, pp. 2864–2880, Oct. 1984, doi: 10.1109/TPAS.1984.318284.

[9] M. Rahli and P. Pirotte, "Optimal load flow using sequential unconstrained minimization technique (SUMT) method under power transmission losses minimization," *Electr. Power Syst. Res.*, vol. 52, no. 1, pp. 61–64, Oct. 1999, doi: 10.1016/s0378-7796(99)00008-5.

[10] X. Yan and V. H. Quintana, "Improving an interior-point-based OPF by dynamic adjustments of step sizes and tolerances," *IEEE Trans. Power Syst.*, vol. 14, no. 2, pp. 709–717, May 1999, doi: 10.1109/59.761902.

[11] D. C. Walters and G. B. Sheble, "Genetic algorithm solution of economic dispatch with valve point loading," *IEEE Trans. Power Syst.*, vol. 8, no. 3, pp. 1325–1332, Mar. 1993, doi: 10.1109/59.260861.

[12] L. L. Lai, J. T. Ma, R. Yokoyama, and M. Zhao, "Improved genetic algorithms for optimal power flow under both normal and contingent operation states," *Int. J. Electr. Power Energy Syst.*, vol. 19, no. 5, pp. 287–292, Jun. 1997, doi: 10.1016/s0142-0615(96)00051-8.

[13] J. Yuryevich and K. Po Wong, "Evolutionary programming based optimal power flow algorithm," *IEEE Trans. Power Syst.*, vol. 14, no. 4, pp. 1245–1250, Apr. 1999, doi: 10.1109/59.801880.

[14] A. G. Bakirtzis, P. N. Biskas, C. E. Zoumas, and V. Petridis, "Optimal power flow by enhanced genetic algorithm," *IEEE Trans. Power Syst.*, vol. 17, no. 2, pp. 229–236, May 2002, doi: 10.1109/TPWRS.2002.1007886.

[15] A. Saini, D. K. Chaturvedi, and A. K. Saxena, "Optimal power flow solution: A GA-fuzzy system approach," *Int. J. Emerg. Electr. Power Syst.*, vol. 5, no. 2, pp. 1–21, Apr. 2006, doi: 10.2202/1553-779x.1091.

[16] M. S. Kumari and S. Maheswarapu, "Enhanced genetic algorithm based computation technique for multi-objective optimal power flow solution," *Int. J. Electr. Power Energy Syst.*, vol. 32, no. 6, pp. 736–742, Jul. 2010, doi: 10.1016/j.ijepes.2010.01.010.

[17] W. Ongsakul and T. Tantimaporn, "Optimal power flow by improved evolutionary programming," *Electric Power Compon. Syst.*, vol. 34, no. 1, pp. 79–95, Jan. 2006, doi: 10.1080/15325000691001458.

[18] A. A. Abou El Ela, M. A. Abido, and S. R. Spea, "Optimal power flow using differential evolution algorithm," *Electr. Power Syst. Res.*, vol. 80, no. 7, pp. 878–885, Jul. 2010, doi: 10.1016/j.epsr.2009.12.018.

[19] C. Thitithamrongchai and B. Eua-arporn, "Self-adaptive differential evolution based optimal power flow for units with non-smooth fuel cost functions," *J. Elect. Syst.*, vol. 3, no. 2, pp. 88–99, 2007.

[20] S. Sayah and K. Zehar, "Modified differential evolution algorithm for optimal power flow with non-smooth cost functions," *Energy Convers. Manage.*, vol. 49, no. 11, pp. 3036–3042, Nov. 2008, doi: 10.1016/j.enconman.2008.06.014.

[21] C. Li, H. Zhao, and T. Chen, "The hybrid differential evolution algorithm for optimal power flow based on simulated annealing and Tabu search," in *Proc. Int. Conf. Manage. Service Sci.*, Aug. 2010, pp. 1–7, doi: 10.1109/ICMSS.2010.5578512.

[22] S. Li, W. Gong, C. Hu, X. Yan, L. Wang, and Q. Gu, "Adaptive constraint differential evolution for optimal power flow," *Energy*, vol. 235, Nov. 2021, Art. no. 121362, doi: 10.1016/j.energy.2021.121362.

[23] P. P. Biswas, P. N. Suganthan, R. Mallipeddi, and G. A. J. Amaratunga, "Optimal power flow solutions using differential evolution algorithm integrated with effective constraint handling techniques," *Eng. Appl. Artif. Intell.*, vol. 68, pp. 81–100, Feb. 2018, doi: 10.1016/j.engappai.2017.10.019.

[24] M. A. Abido, "Optimal power flow using particle swarm optimization," *Int. J. Electr. Power Energy Syst.*, vol. 24, no. 7, pp. 563–571, Oct. 2002, doi: 10.1016/s0142-0615(01)00067-9.

[25] D. B. Attous and Y. Labb, "Particle swarm optimisation based optimal power flow for units with non-smooth fuel cost functions," *Model., Meas. Control A*, vol. 83, nos. 3–4, pp. 377–381, 2010.

[26] T. Niknam, M. R. Narimani, J. Aghaei, and R. Azizipanah-Abarghooee, "Improved particle swarm optimisation for multi-objective optimal power flow considering the cost, loss, emission and voltage stability index," *IET Gener., Transmiss. Distrib.*, vol. 6, no. 6, p. 515, 2012, doi: 10.1049/iet-gtd.2011.0851.

[27] K. Vaisakh, L. R. Srinivas, and K. Meah, "Genetic evolving ant direction particle swarm optimization algorithm for optimal power flow with non-smooth cost functions and statistical analysis," *Appl. Soft Comput.*, vol. 13, no. 12, pp. 4579–4593, Dec. 2013, doi: 10.1016/j.asoc.2013.07.002.

[28] L. D. Le, J. Polprasert, W. Ongsakul, D. N. Vo, and D. A. Le, "Stochastic weight trade-off particle swarm optimization for optimal power flow," *J. Autom. Control Eng.*, vol. 2, no. 1, pp. 31–37, 2014, doi: 10.12720/joace.2.1.31-37.

[29] V. Roberge, M. Tarbouchi, and F. Okou, "Optimal power flow based on parallel metaheuristics for graphics processing units," *Electric Power Syst. Res.*, vol. 140, pp. 344–353, Nov. 2016, doi: 10.1016/j.epsr.2016.06.006.

[30] A. Bhattacharya and P. K. Chattopadhyay, "Application of biogeography-based optimisation to solve different optimal power flow problems," *IET Gener., Transmiss. Distrib.*, vol. 5, no. 1, p. 70, 2011, doi: 10.1049/iet-gtd.2010.0237.

[31] P. K. Roy and D. Mandal, "Quasi-oppositional biogeography-based optimization for multi-objective optimal power flow," *Electr. Power Compon. Syst.*, vol. 40, no. 2, pp. 236–256, Dec. 2011, doi: 10.1080/15325008.2011.629337.

[32] A. Ramesh Kumar and L. Premalatha, "Optimal power flow for a deregulated power system using adaptive real coded biogeography-based optimization," *Int. J. Electr. Power Energy Syst.*, vol. 73, pp. 393–399, Dec. 2015, doi: 10.1016/j.ijepes.2015.05.011.

[33] S. Duman, U. Güvenç, Y. Sönmez, and N. Yörükeren, ''Optimal power flow using gravitational search algorithm,'' *Energy Convers. Manage.*, vol. 59, pp. 86–95, Jul. 2012, doi: 10.1016/j.enconman.2012.02.024.

[34] A. R. Bhowmik and A. K. Chakraborty, ''Solution of optimal power flow using nondominated sorting multi objective gravitational search algorithm,'' *Int. J. Electr. Power Energy Syst.*, vol. 62, pp. 323–334, Nov. 2014, doi: 10.1016/j.ijepes.2014.04.053.

[35] A. R. Bhowmik and A. K. Chakraborty, ''Solution of optimal power flow using non dominated sorting multi objective opposition based gravitational search algorithm,'' *Int. J. Electr. Power Energy Syst.*, vol. 64, pp. 1237–1250, Jan. 2015, doi: 10.1016/j.ijepes.2014.09.015.

[36] S. Sivasubramani and K. S. Swarup, ''Multi-objective harmony search algorithm for optimal power flow problem,'' *Int. J. Electr. Power Energy Syst.*, vol. 33, no. 3, pp. 745–752, Mar. 2011, doi: 10.1016/j.ijepes.2010.12.031.

[37] N. Sinsuphan, U. Leeton, and T. Kulworawanichpong, ''Optimal power flow solution using improved harmony search method,'' *Appl. Soft Comput.*, vol. 13, no. 5, pp. 2364–2374, May 2013, doi: 10.1016/j.asoc.2013.01.024.

[38] R. Arul, G. Ravi, and S. Velusami, ''Solving optimal power flow problems using chaotic self-adaptive differential harmony search algorithm,'' *Electr. Power Compon. Syst.*, vol. 41, no. 8, pp. 782–805, May 2013, doi: 10.1080/15325008.2013.769033.

[39] M. Rezaei Adaryani and A. Karami, ''Artificial bee colony algorithm for solving multi-objective optimal power flow problem,'' *Int. J. Electr. Power Energy Syst.*, vol. 53, pp. 219–230, Dec. 2013, doi: 10.1016/j.ijepes.2013.04.021.

[40] X. He, W. Wang, J. Jiang, and L. Xu, ''An improved artificial bee colony algorithm and its application to multi-objective optimal power flow,'' *Energies*, vol. 8, no. 4, pp. 2412–2437, Mar. 2015, doi: 10.3390/en8042412.

[41] A. Panda and M. Tripathy, ''Optimal power flow solution of wind integrated power system using modified bacteria foraging algorithm,'' *Int. J. Electr. Power Energy Syst.*, vol. 54, pp. 306–314, Jan. 2014, doi: 10.1016/j.ijepes.2013.07.018.

[42] H. R. E. H. Bouchekara, M. A. Abido, and M. Boucherma, ''Optimal power flow using teaching-learning-based optimization technique,'' *Electr. Power Syst. Res.*, vol. 114, pp. 49–59, Sep. 2014, doi: 10.1016/j.epsr.2014.03.032.

[43] S. Ermiş, ''Multi-objective optimal power flow using a modified weighted teaching-learning based optimization algorithm,'' *Electr. Power Compon. Syst.*, vol. 51, no. 20, pp. 2536–2556, Dec. 2023, doi: 10.1080/15325008.2023.2239237.

[44] M. Ghasemi, S. Ghavidel, M. Gitizadeh, and E. Akbari, ''An improved teaching–learning-based optimization algorithm using Lévy mutation strategy for non-smooth optimal power flow,'' *Int. J. Electr. Power Energy Syst.*, vol. 65, pp. 375–384, Feb. 2015, doi: 10.1016/j.ijepes.2014.10.027.

[45] A. A. El-Fergany and H. M. Hasanien, ''Single and multi-objective optimal power flow using grey wolf optimizer and differential evolution algorithms,'' *Electr. Power Compon. Syst.*, vol. 43, no. 13, pp. 1548–1559, Aug. 2015, doi: 10.1080/15325008.2015.1041625.

[46] A. Meng, C. Zeng, P. Wang, D. Chen, T. Zhou, X. Zheng, and H. Yin, ''A high-performance crisscross search based grey wolf optimizer for solving optimal power flow problem,'' *Energy*, vol. 225, Jun. 2021, Art. no. 120211, doi: 10.1016/j.energy.2021.120211.

[47] U. Kılıç, ''Backtracking search algorithm-based optimal power flow with valve point effect and prohibited zones,'' *Electr. Eng.*, vol. 97, no. 2, pp. 101–110, Jun. 2015, doi: 10.1007/s00202-014-0315-0.

[48] S. Duman, ''Symbiotic organisms search algorithm for optimal power flow problem based on valve-point effect and prohibited zones,'' *Neural Comput. Appl.*, vol. 28, no. 11, pp. 3571–3585, Nov. 2017, doi: 10.1007/s00521-016-2265-0.

[49] H. Pulluri, R. Naresh, and V. Sharma, ''A solution network based on stud Krill Herd algorithm for optimal power flow problems,'' *Soft Comput.*, vol. 22, no. 1, pp. 159–176, Jan. 2018, doi: 10.1007/s00500-016-2319-3.

[50] A. Mukherjee and V. Mukherjee, ''Solution of optimal power flow with FACTS devices using a novel oppositional Krill Herd algorithm,'' *Int. J. Electr. Power Energy Syst.*, vol. 78, pp. 700–714, Jun. 2016, doi: 10.1016/j.ijepes.2015.12.001.

[51] M. A. Taher, S. Kamel, F. Jurado, and M. Ebeed, ''An improved moth-flame optimization algorithm for solving optimal power flow problem,'' *Int. Trans. Electr. Energy Syst.*, vol. 29, no. 3, p. e2743, Mar. 2019, doi: 10.1002/etep.2743.

[52] W. Warid, H. Hizam, N. Mariun, and N. Abdul-Wahab, ''Optimal power flow using the Jaya algorithm,'' *Energies*, vol. 9, no. 9, p. 678, Aug. 2016, doi: 10.3390/en9090678.

[53] W. Warid, ''Optimal power flow using the AMTPG-Jaya algorithm,'' *Appl. Soft Comput.*, vol. 91, Jun. 2020, Art. no. 106252, doi: 10.1016/j.asoc.2020.106252.

[54] A.-F. Attia, R. A. El Sehiemy, and H. M. Hasanien, ''Optimal power flow solution in power systems using a novel sine-cosine algorithm,'' *Int. J. Electr. Power Energy Syst.*, vol. 99, pp. 331–343, Jul. 2018, doi: 10.1016/j.ijepes.2018.01.024.

[55] A.-A.-A. Mohamed, Y. S. Mohamed, A. A. M. El-Gaafary, and A. M. Hemeida, ''Optimal power flow using moth swarm algorithm,'' *Electr. Power Syst. Res.*, vol. 142, pp. 190–206, Jan. 2017, doi: 10.1016/j.epsr.2016.09.025.

[56] H. Su, Q. Niu, and Z. Yang, ''Optimal power flow using improved cross-entropy method,'' *Energies*, vol. 16, no. 14, p. 5466, Jul. 2023, doi: 10.3390/en16145466.

[57] A. M. Shaheen, R. A. El-Sehiemy, H. M. Hasanien, and A. Ginidi, ''An enhanced optimizer of social network search for multi-dimension optimal power flow in electrical power grids,'' *Int. J. Electr. Power Energy Syst.*, vol. 155, Jan. 2024, Art. no. 109572, doi: 10.1016/j.ijepes.2023.109572.

[58] N. Guha, Z. Wang, M. Wytock, and A. Majumdar, ''Machine learning for AC optimal power flow,'' 2019, *arXiv:1910.08842*.

[59] J. Rahman, C. Feng, and J. Zhang, ''A learning-augmented approach for AC optimal power flow,'' *Int. J. Electr. Power Energy Syst.*, vol. 130, Sep. 2021, Art. no. 106908, doi: 10.1016/j.ijepes.2021.106908.

[60] A. M. Shaheen, R. A. El-Sehiemy, E. E. Elattar, and A. S. Abd-Elrazek, ''A modified crow search optimizer for solving non-linear OPF problem with emissions,'' *IEEE Access*, vol. 9, pp. 43107–43120, 2021, doi: 10.1109/ACCESS.2021.3060710.

[61] S. A. El-Sattar, S. Kamel, M. Ebeed, and F. Jurado, ''An improved version of salp swarm algorithm for solving optimal power flow problem,'' *Soft Comput.*, vol. 25, no. 5, pp. 4027–4052, Mar. 2021, doi: 10.1007/s00500-020-05431-4.

[62] J.-H. Zhu, J.-S. Wang, X.-Y. Zhang, H.-M. Song, and Z.-H. Zhang, ''Mathematical distribution coyote optimization algorithm with crossover operator to solve optimal power flow problem of power system,'' *Alexandria Eng. J.*, vol. 69, pp. 585–612, Apr. 2023, doi: 10.1016/j.aej.2023.02.023.

[63] M. Ahmad, N. Javaid, I. A. Niaz, I. Ahmed, and M. A. Hashmi, ''An orthogonal learning bird swarm algorithm for optimal power flow problems,'' *IEEE Access*, vol. 11, pp. 23659–23680, 2023, doi: 10.1109/ACCESS.2023.3253796.

[64] M. Premkumar, C. Kumar, T. D. Raj, S. D. T. S. Jebaseelan, P. Jangir, and H. H. Alhelou, ''A reliable optimization framework using ensembled successive history adaptive differential evolutionary algorithm for optimal power flow problems,'' *IET Gener., Transmiss. Distrib.*, vol. 17, no. 6, pp. 1333–1357, Mar. 2023, doi: 10.1049/gtd2.12738.

[65] W. Yi, Z. Lin, Y. Lin, S. Xiong, Z. Yu, and Y. Chen, ''Solving optimal power flow problem via improved constrained adaptive differential evolution,'' *Mathematics*, vol. 11, no. 5, p. 1250, Mar. 2023, doi: 10.3390/math11051250.

[66] M. Kaur and N. Narang, ''Optimal power flow solution using space transformational invasive weed optimization algorithm,'' *Iranian J. Sci. Technol., Trans. Electr. Eng.*, vol. 47, no. 3, pp. 939–965, Sep. 2023, doi: 10.1007/s40998-023-00592-y.

[67] A. M. Shaheen, R. A. El-Sehiemy, M. M. Alharthi, S. S. M. Ghoneim, and A. R. Ginidi, ''Multi-objective jellyfish search optimizer for efficient power system operation based on multi-dimensional OPF framework,'' *Energy*, vol. 237, Dec. 2021, Art. no. 121478, doi: 10.1016/j.energy.2021.121478.

[68] V. Bathina, R. Devarapalli, and F. P. G. Márquez, ''Hybrid approach with combining cuckoo-search and grey-wolf optimizer for solving optimal power flow problems,'' *J. Electr. Eng. Technol.*, vol. 18, no. 3, pp. 1637–1653, May 2023, doi: 10.1007/s42835-022-01301-1.

[69] R. Keswani, H. K. Verma, and S. K. Sharma, ''Multi-objective optimal power flow employing a hybrid sine cosine–grey wolf optimizer,'' *Iranian J. Sci. Technol., Trans. Electr. Eng.*, vol. 47, no. 4, pp. 1365–1388, Dec. 2023, doi: 10.1007/s40998-023-00631-8.

[70] M. Ahmadipour, M. M. Othman, R. Bo, M. S. Javadi, H. M. Ridha, and M. Alrifaey, ''Optimal power flow using a hybridization algorithm of arithmetic optimization and Aquila optimizer,'' *Expert Syst. Appl.*, vol. 235, Jan. 2024, Art. no. 121212, doi: 10.1016/j.eswa.2023.121212.

[71] S. S. Reddy, "Optimal power flow using hybrid differential evolution and harmony search algorithm," *Int. J. Mach. Learn. Cybern.*, vol. 10, no. 5, pp. 1077–1091, May 2019, doi: 10.1007/s13042-018-0786-9.

[72] E. Naderi, M. Pourakbari-Kasmaei, F. V. Cerna, and M. Lehtonen, "A novel hybrid self-adaptive heuristic algorithm to handle single- and multi-objective optimal power flow problems," *Int. J. Electr. Power Energy Syst.*, vol. 125, Feb. 2021, Art. no. 106492, doi: 10.1016/j.ijepes.2020.106492.

[73] T. T. Nguyen, "A high performance social spider optimization algorithm for optimal power flow solution with single objective optimization," *Energy*, vol. 171, pp. 218–240, Mar. 2019, doi: 10.1016/j.energy.2019.01.021.

[74] M. Ebeed, M. A. Abdelmotaleb, N. H. Khan, R. Jamal, S. Kamel, A. G. Hussien, H. M. Zawbaa, F. Jurado, and K. Sayed, "A modified artificial hummingbird algorithm for solving optimal power flow problem in power systems," *Energy Rep.*, vol. 11, pp. 982–1005, Jun. 2024, doi: 10.1016/j.egyr.2023.12.053.

[75] S. P. Dash, K. R. Subhashini, and P. Chinta, "Development of a boundary assigned animal migration optimization algorithm and its application to optimal power flow study," *Expert Syst. Appl.*, vol. 200, Aug. 2022, Art. no. 116776, doi: 10.1016/j.eswa.2022.116776.

[76] H. Tazvinga, B. Zhu, and X. Xia, "Optimal power flow management for distributed energy resources with batteries," *Energy Convers. Manage.*, vol. 102, pp. 104–110, Sep. 2015, doi: 10.1016/j.enconman.2015.01.015.

[77] H. M. Dubey, M. Pandit, and B. K. Panigrahi, "Hybrid flower pollination algorithm with time-varying fuzzy selection mechanism for wind integrated multi-objective dynamic economic dispatch," *Renew. Energy*, vol. 83, pp. 188–202, Nov. 2015, doi: 10.1016/j.renene.2015.04.034.

[78] E. E. Elattar, "Optimal power flow of a power system incorporating stochastic wind power based on modified moth swarm algorithm," *IEEE Access*, vol. 7, pp. 89581–89593, 2019, doi: 10.1109/ACCESS.2019.2927193.

[79] K. Dasgupta, P. K. Roy, and V. Mukherjee, "Power flow based hydro-thermal-wind scheduling of hybrid power system using sine cosine algorithm," *Electr. Power Syst. Res.*, vol. 178, Jan. 2020, Art. no. 106018, doi: 10.1016/j.epsr.2019.106018.

[80] S. R. Salkuti, "Optimal power flow using multi-objective glowworm swarm optimization algorithm in a wind energy integrated power system," *Int. J. Green Energy*, vol. 16, no. 15, pp. 1547–1561, Dec. 2019, doi: 10.1080/15435075.2019.1677234.

[81] T. Niknam, M. R. Narimani, and R. Azizipanah-Abarghooee, "A new hybrid algorithm for optimal power flow considering prohibited zones and valve point effect," *Energy Convers. Manage.*, vol. 58, pp. 197–206, Jun. 2012, doi: 10.1016/j.enconman.2012.01.017.

[82] O. Alsac and B. Stott, "Optimal load flow with steady-state security," *IEEE Trans. Power App. Syst.*, vol. PAS-93, no. 3, pp. 745–751, May 1974, doi: 10.1109/TPAS.1974.293972.

[83] R. D. Zimmerman and C. E. Murillo-Sánchez, Oct. 2020, "MATPOWER," *Zenodo*, doi: 10.5281/zenodo.4074135.

[84] *Appendix—A Data for IEEE-30 Bus Test System*, IEEE, Piscataway, NJ, USA, 1961.

[85] P. P. Biswas, P. N. Suganthan, and G. A. J. Amaratunga, "Optimal power flow solutions incorporating stochastic wind and solar power," *Energy Convers. Manage.*, vol. 148, pp. 1194–1207, Sep. 2017, doi: 10.1016/j.enconman.2017.06.071.

[86] R. Jamal, J. Zhang, B. Men, N. H. Khan, M. Ebeed, T. Jamal, and E. A. Mohamed, "Chaotic-quasi-oppositional-phasor based multi populations gorilla troop optimizer for optimal power flow solution," *Energy*, vol. 301, Aug. 2024, Art. no. 131684, doi: 10.1016/j.energy.2024.131684.

[87] T. Niknam, M. R. Narimani, M. Jabbari, and A. R. Malekpour, "A modified shuffle frog leaping algorithm for multi-objective optimal power flow," *Energy*, vol. 36, no. 11, pp. 6420–6432, Nov. 2011, doi: 10.1016/j.energy.2011.09.027.

[88] I. Peña, C. B. Martinez-Anido, and B.-M. Hodge, "An extended IEEE 118-bus test system with high renewable penetration," *IEEE Trans. Power Syst.*, vol. 33, no. 1, pp. 281–289, Jan. 2018, doi: 10.1109/TPWRS.2017.2695963.

[89] Z. Yetgin and M. Şamdan, "Honey formation optimization: HFO," *Turkish J. Eng.*, vol. 5, no. 2, pp. 81–88, Apr. 2021, doi: 10.31127/tuje.693103.

[90] Z. Yetgin and U. Ercan, "Honey formation optimization with single component for numerical function optimization: HFO-1," *Neural Comput. Appl.*, vol. 35, no. 35, pp. 24897–24923, Dec. 2023, doi: 10.1007/s00521-023-08984-1.

[91] K. Abaci and V. Yamacli, "Differential search algorithm for solving multi-objective optimal power flow problem," *Int. J. Electr. Power Energy Syst.*, vol. 79, pp. 1–10, Jul. 2016, doi: 10.1016/j.ijepes.2015.12.021.

[92] Z. Yetgin and H. Abaci, "Honey formation optimization framework for design problems," *Appl. Math. Comput.*, vol. 394, Apr. 2021, Art. no. 125815, doi: 10.1016/j.amc.2020.125815.

[93] H. Saadat, *Power System Analysis* (Systems, Controls, Embedded Systems, Energy, and Machines), vol. 3, 3rd ed., Alexandria, VA, USA: PSA Publishing LLC, 2011.

[94] E. Naderi, M. Pourakbari-Kasmaei, and H. Abdi, "An efficient particle swarm optimization algorithm to solve optimal power flow problem integrated with FACTS devices," *Appl. Soft Comput.*, vol. 80, pp. 243–262, Jul. 2019, doi: 10.1016/j.asoc.2019.04.012.

[95] C. V. Suresh and S. Sivanagaraju, "Analysis and effect of multi-fuel and practical constraints on economic load dispatch in the presence of unified power flow controller using UDTPSO," *Ain Shams Eng. J.*, vol. 6, no. 3, pp. 803–817, Sep. 2015, doi: 10.1016/j.asej.2014.12.011.

[96] M. A. Abido, "Optimal power flow using Tabu search algorithm," *Electr. Power Compon. Syst.*, vol. 30, no. 5, pp. 469–483, May 2002, doi: 10.1080/15325000252888425.

[97] M. Balasubbareddy, S. Sivanagaraju, and C. V. Suresh, "Multi-objective optimization in the presence of practical constraints using non-dominated sorting hybrid cuckoo search algorithm," *Eng. Sci. Technol., Int. J.*, vol. 18, no. 4, pp. 603–615, Dec. 2015, doi: 10.1016/j.jestch.2015.04.005.

[98] R. Gnanadass, N. P. Padhy, and K. Manivannan, "Assessment of available transfer capability for practical power systems with combined economic emission dispatch," *Electr. Power Syst. Res.*, vol. 69, nos. 2–3, pp. 267–276, May 2004, doi: 10.1016/j.epsr.2003.10.007.

[99] N. Daryani, M. T. Hagh, and S. Teimourzadeh, "Adaptive group search optimization algorithm for multi-objective optimal power flow problem," *Appl. Soft Comput.*, vol. 38, pp. 1012–1024, Jan. 2016, doi: 10.1016/j.asoc.2015.10.057.

[100] M. R. Narimani, R. Azizipanah-Abarghooee, B. Zoghdar-Moghadam-Shahrekohne, and K. Gholami, "A novel approach to multi-objective optimal power flow by a new hybrid optimization algorithm considering generator constraints and multi-fuel type," *Energy*, vol. 49, pp. 119–136, Jan. 2013, doi: 10.1016/j.energy.2012.09.031.

[101] A. Saha, P. Das, and A. K. Chakraborty, "Water evaporation algorithm: A new metaheuristic algorithm towards the solution of optimal power flow," *Eng. Sci. Technol., Int. J.*, vol. 20, no. 6, pp. 1540–1552, Dec. 2017, doi: 10.1016/j.jestch.2017.12.009.

[102] Z. Ullah, S. Wang, J. Radosavljevic, and J. Lai, "A solution to the optimal power flow problem considering WT and PV generation," *IEEE Access*, vol. 7, pp. 46763–46772, 2019, doi: 10.1109/ACCESS.2019.2909561.

[103] A. Ali, A. Hassan, M. U. Keerio, N. H. Mugheri, G. Abbas, M. Hatatah, E. Touti, and A. Yousef, "A novel solution to optimal power flow problems using composite differential evolution integrating effective constrained handling techniques," *Sci. Rep.*, vol. 14, no. 1, p. 6187, Mar. 2024, doi: 10.1038/s41598-024-56590-5.

[104] T. P. Chang, "Investigation on frequency distribution of global radiation using different probability density functions," *Int. J. Appl. Sci. Eng.*, vol. 8, no. 2, pp. 99–107, 2010.

[105] L. Shi, C. Wang, L. Yao, Y. Ni, and M. Bazargan, "Optimal power flow solution incorporating wind power," *IEEE Syst. J.*, vol. 6, no. 2, pp. 233–241, Jun. 2012, doi: 10.1109/JSYST.2011.2162896.

[106] S. Mouassa, A. Althobaiti, F. Jurado, and S. S. M. Ghoneim, "Novel design of slim mould optimizer for the solution of optimal power flow problems incorporating intermittent sources: A case study of Algerian electricity grid," *IEEE Access*, vol. 10, pp. 22646–22661, 2022, doi: 10.1109/ACCESS.2022.3152557.

[107] M. Farhat, S. Kamel, A. M. Atallah, and B. Khan, "Optimal power flow solution based on jellyfish search optimization considering uncertainty of renewable energy sources," *IEEE Access*, vol. 9, pp. 100911–100933, 2021, doi: 10.1109/ACCESS.2021.3097006.

[108] S. Mouassa, A. Alateeq, A. Alassaf, R. Bayindir, I. Alsaleh, and F. Jurado, "Optimal power flow analysis with renewable energy resource uncertainty using dwarf mongoose optimizer: Case of ADRAR isolated electrical network," *IEEE Access*, vol. 12, pp. 10202–10218, 2024, doi: 10.1109/ACCESS.2024.3351721.

[109] M. H. Sulaiman and Z. Mustaffa, "Optimal power flow incorporating stochastic wind and solar generation by metaheuristic optimizers," *Microsyst. Technol.*, vol. 27, no. 9, pp. 3263–3277, Sep. 2021, doi: 10.1007/s00542-020-05046-7.

[110] N. A. Nguyen, D. N. Vo, T. T. Nguyen, and T. L. Duong, "An improved equilibrium optimizer algorithm for solving optimal power flow problem with penetration of wind and solar energy," *Int. Trans. Electr. Energy Syst.*, vol. 2022, pp. 1–21, Jun. 2022, doi: 10.1155/2022/7827164.

VOLKAN YAMAÇLI received the B.Sc. degree in electrical-electronics engineering from Mersin University, Mersin, Türkiye, and the M.Sc. and Ph.D. degrees in electrical-electronics engineering from the Institute of Applied Sciences, Mersin University. He is currently an Assistant Professor with the Department of Computer Engineering, Mersin University. His current research interests include hybrid power and energy systems, deep learning, and artificial intelligence solutions.

HAKAN IŞIKER (Member, IEEE) received the Ph.D. degree in electrical and electronics engineering from Mersin University, Mersin, Türkiye, in 2020.

He is currently an Assistant Professor with the Electrical and Electronics Engineering Department, Mersin University. He is the author or co-author of more than 20 publications in journals and conferences. His research interests include passive radar imaging systems, synthetic aperture radar (SAR) focusing algorithms, image processing, target detection techniques, optimization, and artificial intelligence algorithms.

ZEKİ YETGİN received the B.Sc. and M.Sc. degrees from the Computer Engineering Department, Eastern Mediterranean University, Cyprus, in 1999 and 2002, respectively, and the Ph.D. degree from the Department of Computer Engineering, Dokuz Eylul University, Izmir, Türkiye, in 2008. He was an Associate Professor, in 2014, and promoted to a Professor, in 2020. He is currently a Professor with the Department of Computer Engineering, Mersin University. His research interests include machine learning, optimization, networks, and multimedia. He is particularly involved in honey formation optimization, computer vision, and QoE of multimedia services.

KADİR ABACI received the B.Sc. degree in electrical and electronics engineering from Istanbul Technical University, in 1993, and the M.Sc. and Ph.D. degrees in electrical and electronics engineering from Sakarya University, in 2003 and 2007, respectively. He is a Professor of Electrical and Electronics Engineering at Mersin University. He has done academic work in the Mersin University. The author has more than 50 publications, including original publications and conferences. His research, mostly in the field of voltage stability of the power systems, power system optimization, and its control applications.